SANDIA REPORT

SAND99-2104
Unlimited Release
Printed September 1999

Multimechanism-Deformation Parameters of Domal Salts Using Transient Creep Analysis

Darrell E. Munson

Prepared by
Sandia National Laboratories
Albuquerque, New Mexico 87185 and Livermore, California 94550

Sandia is a multiprogram laboratory operated by Sandia Corporation, a Lockheed Martin Company, for the United States Department of Energy under Contract DE-AC04-94AL85000.

Sandia National Laboratories

Issued by Sandia National Laboratories, operated for the United States Department of Energy by Sandia Corporation.

Available to DOE and DOE contractors from
Office of Scientific and Technical Information
P.O. Box 62
Oak Ridge, TN 37831

Prices available from (703) 605-6000
Web site: http://www.ntis.gov/ordering.htm

Available to the public from
National Technical Information Service
U.S. Department of Commerce
5285 Port Royal Rd
Springfield, VA 22161

NTIS price codes
Printed copy: A03
Microfiche copy: A01

DISCLAIMER

Portions of this document may be illegible in electronic image products. Images are produced from the best available original document.

SAND99-2104
Unlimited Release
Printed September 1999

MULTIMECHANISM-DEFORMATION PARAMETERS OF DOMAL SALTS USING TRANSIENT CREEP ANALYSIS

Darrell E. Munson
Underground Storage Technology Department
Sandia National Laboratories
P.O. Box 5800
Albuquerque, NM 87185-0706

ABSTRACT

Use of Gulf Coast salt domes for construction of very large storage caverns by solution mining has grown significantly in the last several decades. In fact, among the largest developers of storage caverns along the Gulf Coast is the Strategic Petroleum Reserve (SPR) which has purchased or constructed 62 crude oil storage caverns in four storage sites (domes). Although SPR and commercial caverns have been operated economically for many years, the caverns still exhibit some relatively poorly understood behaviors, especially involving creep closure volume loss and hanging string damage from salt falls. Since it is possible to postulate that some of these behaviors stem from geomechanical or deformational aspects of the salt, a method of correlating the cavern response to mechanical creep behavior as determined in the laboratory could be of considerable value. Recently, detailed study of the creep response of domal salts has cast some insight into the influence of different salt origins on cavern behavior. The study used a simple graphical analysis of limited non-steady state data to establish an approach or bound to steady state, as an estimate of the steady state behavior of a given salt. This permitted analysis of sparse creep databases for domal salts. It appears that a shortcoming of this steady state analysis method is that it obscures some critical differences of the salt material behavior. In an attempt to overcome the steady state analysis shortcomings, a method was developed based on integration of the Multimechanism-Deformation (M-D) creep constitutive model to obtain fits to the transient response. This integration process permits definition of all the material sensitive parameters of the model, while those parameters that are constants or material insensitive parameters are fixed independently. The transient analysis method has proven more sensitive to differences in the creep characteristics and has provided a way of defining different behaviors within a given dome. Characteristics defined by the transient analysis are related quantitatively to the volume loss creep rate of the SPR caverns. This increase in understanding of the domal material creep response already has pointed to the possibility of delineating the existence of material spines within a specific dome. Further definition of the domal geology and structure seems possible only through expansion of the creep databases for domal salts.

ACKNOWLEDGMENTS

The author would like to acknowledge the continued support of Bob Myers, DOE SPR/PMO who initiated the study of hanging string damage and the behavior of cavern salt materials, of which this report is a part. Also the support of Jim Linn, who leads the SPR Program at Sandia National Laboratories, is highly valued. The reviews by Bob Myers, Arlo Fossum, and Brian Ehgartner are greatly appreciated, as are the significant comments by Nancy Brodsky on a related work.

CONTENTS

FIGURES

TABLES

1.0 INTRODUCTION

Often in major geotechnical construction projects, geotechnical data availability may be quite limited because of both financial and time constraints. As a consequence, it is essential that the use of these limited data be optimized. This implies the need for analysis procedures that extract as much information as possible from the available databases. Such an optimization of data analysis has proven possible in the sparse databases for mechanical creep behavior of salt specimens taken from salt domes. It is in these domes that the construction of massive storage caverns is relatively common. To some extent, the knowledge provided by the data analysis is retrospective since the domal salt site acquisition and cavern construction normally begins prior to any possible availability of geomechanical testing of specimens. However, extant collections of data from a given dome or domal site could be instructive in future cavern site acquisition and construction. Moreover, even post construction knowledge of domal salt response may prove beneficial to the understanding of differences in cavern behavior and operation characteristics.

A basis for the steady state analysis of sparse creep databases was established in an earlier work [Munson, 1998]. This analysis was aimed at determining the steady state creep rate from limited amounts of either conventional or incremental creep data. A conventional creep test is one performed at a constant stress and temperature; whereas, an incremental test consists of several distinct time intervals, each separated by step-wise changes in either stress or temperature, all on the same specimen. Fundamentally, the common framework for behavior of salt is the micromechanical mechanisms controlling creep deformation. This framework, in fact, governs the functional forms of the equations of creep. A well-documented constitutive model that formalizes this behavior is the Multimechanism-Deformation (M-D) model [Munson and Dawson, 1982; Munson et al., 1989; Munson, 1997]. Within this framework, the only real differentiation permitted among salt materials is in the values of just a few of the parameters of the model. All other parameters of the model are either physically determined constants or material insensitive values. As will be illustrated later, the parameters sensitive to different salt materials are (1) the steady state creep parameters, (2) a measure that governs the amount of transient creep, and (3) a measure that controls the rate of change (curvature) of the transient creep. Because the steady state creep parameters are the most obvious of the important material parameters, these parameters were the first to be studied. The functional form of the model was used by Munson [1998] to suggest that any set of creep rates obtained from testing of a given uniform material will determine a bound that approaches the steady state rate. This bound is independent of the type of creep test, conventional or incremental, and depends only on the specimen material. The database of creep results used to determine the bound cannot, however, include incremental stress drop data; these increments must be ignored. Using this rule, it was possible to determine the steady state bounds for seven domal salts where creep results were available. As a result of the steady state analysis, a marked difference was found between the creep rates of the salt of the various domes. In fact, two distinct types of salt creep behaviors were identified: creep resistant (hard) salt and less creep resistant (soft) salt. The steady state rate of the soft salt was some forty times greater than the hard salt.

While this alone is an extremely interesting result, it was made more so through a comparison to a quantification of creep volume loss rates from creep closure of caverns based on field data.

Cavern closure rates were determined for the caverns of the Strategic Petroleum Reserve (SPR) based on field data accumulated over nearly a decade of operation. Creep closure is the primary cause of gradual cavern pressure increase with time. The relatively quiescent caverns of the SPR are routinely monitored for pressure build-up, and periodically bled-down as necessary to maintain the proper operating pressure range. Based on these data, a technology was developed centered on the M-D model to track these operational pressure variations and to separate expected pressure build-up response from abnormal cavern pressure behavior [Ehgartner et al., 1995]. The technology, in the form of a numerical program called CAVEMAN, determines, from best fits to historical data, four cavern related material, shape, and stress parameters, which can then be used to extrapolate expected future cavern pressure response. Because the pressure build-up is primarily related directly to volume closure of the cavern, effective cavern creep rates can be obtained. Exceptional reproduction of cavern histories and the success in extrapolation of future cavern response suggests that the closure rates are accurately determined. When results of the independent steady state analysis of the SPR sites were compared to the CAVEMAN cavern creep rates, it was clear in most cases that at least a crude correlation existed between the steady states rates determined in the laboratory and the cavern creep rates. However, the comparison also highlighted discrepancies that uncovered defects in the steady state analysis method.

Within a given dome, the CAVEMAN results for individual cavern creep responses can show a range of closure rates not predicted by the simple results of the steady state analysis. The rules established for the analysis and the use of all of the creep data for a given dome combine to cause the steady state rate of the most creep resistant salt of the dome to dominate the analysis. In other words, if one of the caverns, or actually one of the wells, has a salt with a higher steady state rate, caverns with more resistant salt will mask its behavior. Also, because the bound only approaches the steady state rate, it is possible to establish an erroneously high value for the steady state. Both of these analysis defects can be corrected, in part, through a more extensive analysis procedure involving integration of both the transient and steady state portions of the model to fit the creep data. For simplicity this will be called a transient analysis.

The purpose of this work is to develop the methodology for transient analysis of salt creep databases, to utilize the analysis for the domal salts, and to compare the results to cavern creep closure rates. This process is initiated by developing the transient analysis framework based on the M-D model of creep [Munson et al., 1989]. This is followed by the procedure used to integrate the model and the scheme for the actual analysis. The results of the transient analysis are presented, together with fits to the creep curves using the three material sensitive parameters. Implications are discussed of the manner in which the values of the three parameters change with stress and temperature. After discussions of the comparisons to the cavern creep closure results and the implications on the geological structure of salt domes, some final remarks summarize the work.

2.0 MULTIMECHANISM-DEFORMATION MODEL

In order to visualize the transient analysis methodology, it is beneficial to begin with a schematic of a raw conventional creep curve, as shown in Figure 1. This creep curve would result from a creep test in which a specimen is loaded at constant stress and temperature and the creep strain recorded as a function of time. Typically, the required rezeroing of the strain at the time of loading would eliminate any instantaneous loading strain. As the schematic illustrates, the total creep strain can be artificially separated into steady state strain, ε_s, and transient strain, ε_t, components. As indicated, the steady state strain grows at a constant rate. However, the evolutionary process controlling the transient strain causes a diminishing rate with continued straining, which eventually becomes zero at some maximum strain value given by the transient strain limit, ε^*_t. Thereafter, further strain accumulates only at the steady state creep rate. Provided it is the initial loading of a virgin (previously undeformed) specimen, the transient is the primary stage of creep. Often, and for various reasons, usually cost, creep tests are terminated in the primary stage of creep, well before the development of steady state creep. Fortunately, as is apparent, the steady state creep contribution is unique to a given creep curve, as is the transient contribution. This uniqueness makes the fitting, even of abbreviated portions of the primary transient, although difficult, entirely possible. It also permits fitting of the constant stress and temperature increments of an incremental test.

Even though the above description is sufficient to properly visualize the transient analysis method, some additional information is necessary to interpret the more complicated incremental creep tests. Plotting the time differential (instantaneous strain rate) of a conventional creep curve of Figure 1 against the amount of transient strain, ε_t (here in terms of the internal state parameter, ζ), one of the curves of Figure 2 would result. In Figure 2, several curves, each at constant stress, of the family of such curves are shown. Incremental creep tests impose different stress loading and temperature conditions for various time intervals successively on the same specimen. Each increment may have transient behavior that the model accounts for through the evolution of the state parameter. A hypothetical incremental test is illustrated in Figure 2, where specimen history follows the appropriate curve for the initial stress, σ_1, and temperature, T_1, with the strain rate decreasing with increasing state parameter magnitude. An abrupt change in stress causes the material to move, with the current state parameter magnitude, to another curve appropriate to the new stress. Again the strain rate moves along this curve until another change in conditions occurs. For strain rate states above steady state (abscissa axis), the material is workhardening (increasing state parameter values). For states below the steady state, the material is in recovery (decreasing state parameter values). The state parameter always moves toward the steady state condition, which occurs when the state parameter, ζ, is equal to ε^*_t. Depending upon the magnitude and direction of the stress or temperature change, the transient may represent material in either workhardening or recovery. The details of the workhardening or recovery processes govern the curvature, or time rate of change, of the transient behavior.

We have now defined the three fundamental features of a creep curve that must be described if a curve is to be fitted: (1) the steady state creep rate, (2) the transient strain

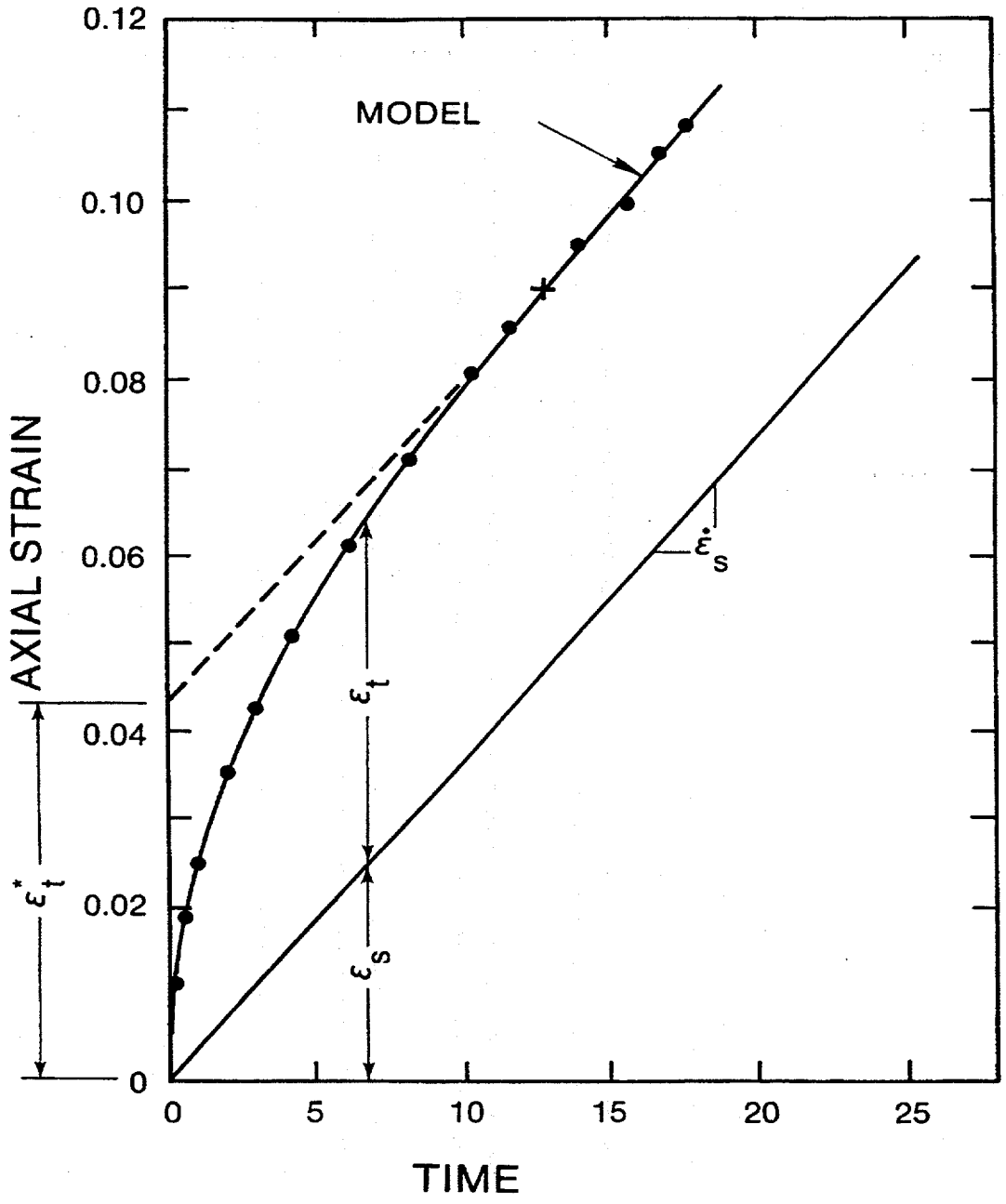

Figure 1. Separation into Steady State and Transient Creep Components.

limit, and (3) the workhardening or recovery time rate of change (curvature). The analysis method used in this work is based on an exact fitting of conventional and incremental creep curves. Such analysis is necessitated by the very limited amount of data available for any one material. In fact, the analysis method essentially makes use all of the points along the entire single creep curve to define the parameters. In contrast, the more conventional analysis method is to use a much larger database to determine the individual parameters by compiling values of the parameters from many specimens to determine not only the appropriate value but also the uncertainty. The difference in the

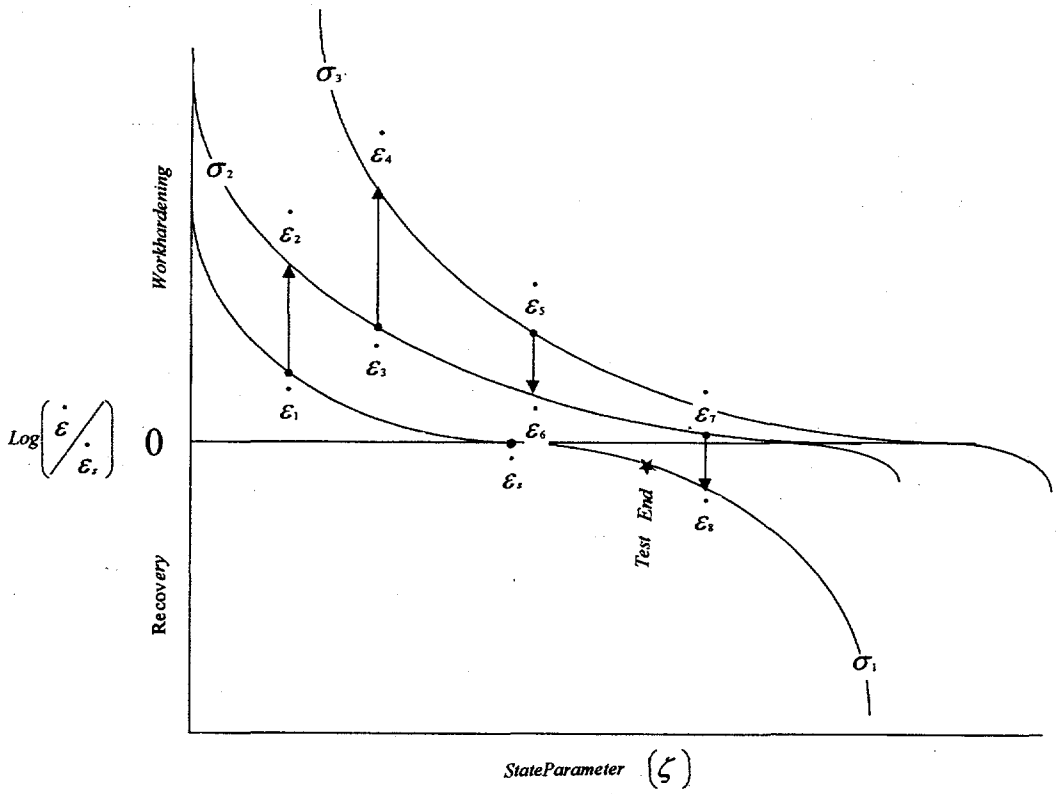

Figure 2. Transient Curves Showing Incremental Test [Munson and Dawson, 1982].

two methods is that both the material and testing uncertainty cannot be determined in the transient analysis because it inherently involves only one specimen. As a consequence, it must be understood that the transient analysis of sparse databases carries a potential risk of unrecognized uncertainty.

With the general concept in mind, we can now develop the mathematical descriptions that make up the M-D constitutive model [Munson, 1997] of salt creep. Through these mathematical equations, it is possible to define all of the necessary material parameters. However, as with any constitutive model, there are some restrictions that define the ranges over which the model is accurate. In developing the constitutive description, only the temperature and stress ranges encountered in mining and storage cavern operations must be addressed. Typically these are low temperature and low to moderately high stresses. For these conditions, creep is envisioned as arising from contributions of three appropriate micromechanical mechanisms as determined from the deformation mechanism-map [Munson, 1979]. These mechanisms are (1) a dislocation climb controlled creep mechanism at high temperatures and low stresses, (2) an empirically specified but undefined mechanism at low temperatures and low stresses, and (3) a dislocation slip controlled mechanism at high stresses [Munson et al., 1989]. Each of these mechanisms is thermally activated, which defines the form of the temperature dependence. The respective steady state creep rates for the three individual mechanisms are given by:

$$\dot{\varepsilon}_{S_1} = A_1 e^{\frac{-Q_1}{RT}} \left(\frac{\sigma}{\mu(1-\omega)} \right)^{n_1}$$

$$\dot{\varepsilon}_{S_2} = A_2 e^{\frac{-Q_2}{RT}} \left(\frac{\sigma}{\mu(1-\omega)} \right)^{n_2} \qquad 1$$

$$\dot{\varepsilon}_{S_3} = \left| H(\sigma - \sigma_0) \right| \left(B_1 e^{\frac{-Q_1}{RT}} + B_2 e^{\frac{-Q_2}{RT}} \right) \sinh \left[\frac{q\left(\frac{\sigma}{1-\omega} - \sigma_0 \right)}{\mu} \right]$$

where the numerical subscripts refer to the appropriate mechanism, the A's and B's are structure factors, Q's are activation energies, R is the universal gas constant, T is the absolute temperature, μ is the shear modulus, q is the stress constant, σ_0 is a stress limit, and H is a Heaviside step function with argument $(\sigma - \sigma_0)$. Here, although not used in the analysis, ω is the continuum damage [Chan et. al., 1998]. It has been shown [Munson et al., 1989] through multiaxial experiments that the proper flow law, or equivalent stress measure, is of the Tresca form, $\sigma = |\sigma_1 - \sigma_3|$, in terms of principal stresses.

These mechanisms act in parallel, which means the individual steady state creep rates can be summed over the three mechanisms to give the total steady state creep rate, as follows:

$$\dot{\varepsilon}_S = \sum_{i=1}^{3} \dot{\varepsilon}_{S_i} \qquad 2$$

The mathematical form of Eqs. 1 and 2 is very important in that they are dependent only on the mechanisms, and these mechanisms are identical for every salt material. We have made use of this fact in the earlier steady state analysis methodology [Munson, 1998] and will use again in the transient analysis. The fitting parameters required for the transient analysis are the structure factors, A's and B's.

The equivalent total strain rate is treated through a multiplier, F, on the steady state rate, as given by

$$\dot{\varepsilon}_{eq} = F \dot{\varepsilon}_s \qquad 3$$

where the multiplier, F, essentially describes the transient response, or more specifically the curvature of the transient response. As noted earlier, the curvature of the transient response of the creep must be described by the fitting routine. The multiplier, F, consists of higher order kinetic functions that define the three branches of the function. Specifically, these branches are the representations of workhardening, steady state, and recovery, as follows:

$$F = \begin{cases} e^{\Delta\left(\left(1-\frac{\zeta}{\varepsilon_t^*}\right)^2\right)} & ; \ \zeta < \varepsilon_t^* \\ 1 & ; \ \zeta = \varepsilon_t^* \\ e^{-\delta\left(\left(1-\frac{\zeta}{\varepsilon_t^*}\right)^2\right)} & ; \ \zeta > \varepsilon_t^* \end{cases} \quad 4$$

Here, Δ is the workhardening parameter, δ is the recovery parameter, ζ is the state parameter, and ε^*_t is the transient strain limit. It is important to note that Eq. 4 defines the curvature as well as the strain magnitude of the transients in the creep curve. The strain magnitude is determined by ε^*_t, and the curvature is defined by Δ or δ, depending upon whether the transient is workhardening or recovering.

The kinetic equation for the state parameter is given by

$$\dot{\zeta} = (F-1)\dot{\varepsilon}_s \quad 5$$

The transient strain limit is defined by

$$\varepsilon_t^* = K_0 e^{cT}\left(\frac{\sigma}{\mu(1-\omega)}\right)^m \quad 6$$

where K_0 and c are constants and m is a theoretical constant. In terms of the transient analysis, the fitting parameter of interest is K_0.

The workhardening, Δ, and recovery, δ, parameters are described through linear functions, as follows:

$$\Delta = \alpha_w + \beta_w \log\left(\frac{\sigma}{\mu(1--\omega)}\right)$$
$$\delta = \alpha_r + \beta_r \log\left(\frac{\sigma}{\mu(1-\omega)}\right) \quad 7$$

where the α's and β's are constants. Here, the fitting parameter for the curvature is either α_w or α_r. It is possible to simplify the fitting process because in this work the recovery parameter is taken as constant, resulting in just one remaining parameter, α_w (or more simply just α).

A total of 17 parameters must be evaluated, not counting the damage parameter and the elastic constants. However, a number of the parameters are constants obtained from "outside" physical processes, while others are material insensitive.

In the earlier work, Munson [1998] discussed the implications of a model based on micromechanical mechanisms. Fundamentally, salt creep behavior has common micromechanical constitutive features regardless of the origin of the salt. All that differs is the exact value of the parameters. In particular, those critical parameters that primarily distinguish one salt material from another are the steady state responses as represented by the structure factors (A's and B's) and the transient strain rate limits (ε^*_t) as represented by K_0. And, although perhaps not quite as critical as the other two material sensitive parameters, the remaining material sensitive parameter, Δ, is represented by α. The companion parameter to Δ, although not really significant in this analysis, is δ, which represents the curvature of the recovery process. Again, as stated previously, the recovery parameter is taken essentially as constant. It has been demonstrated [Munson and Dawson, 1982] that most of the actual situations are stress loading and do not involve recovery. Furthermore, in unloading situations the strain rates become so small that the exact value of δ is experimentally insensitive.

As noted previously, the remaining M-D model parameters are either independent of the exact salt material being considered or are insensitive to material variations. This results from the fact that many of these parameters are related to the salt physical properties and processes at an atomic level. This is a consequence of the micromechanical mechanisms of self-diffusion controlled dislocation climb and dislocation interactions during slip. The activation energies, Q, are related to atomic diffusion processes and, therefore, are not physically sensitive to the origin of the various salt materials. Similarly, the stress exponents, n, are also related to local atomic processes and are insensitive to different salt materials. In this case we can be quite certain based on the physical models that describe them that the values of these parameters do not change. As a result, the same precise values of Q's and n's that were determined for Waste Isolation Pilot Plant (WIPP) clean salt [Munson et al., 1989] will be used for the domal salts. Although, values of the stress limit, σ_0, and the stress constant, q, are, in general, somewhat sensitive to the salt material, here, because of the limited upper stress range of data, they are probably not markedly so. As a consequence, the values of these parameters, σ_0 and q, determined from the WIPP clean salt will also be used for the domal salts. The value of m is a theoretical constant, independent of material. The non-critical value of c is related to an activation process and is assumed to remain unchanged with different materials.

Impurities in the salt material, provided they are identifiable non-coherent separate phases in the salt, do not normally affect the creep parameters significantly. A small change in the structure factors occurs [Munson et al., 1989] through an effective reduction in the stressed area to cause an increase of the salt creep. This is similar to that effect caused by damage, as contained in the previous equations. However, the principal effect of these impurities [Chan et al., 1996] in the damage model is to alter the fracture behavior, not the creep behavior.

3.0 ANALYSIS METHODOLOGY

In the earlier work [Munson, 1998], the M-D model was used in the analysis in a passive sense, specifying only the form of the steady state creep response with stress and temperature. The approach was based upon the fact that the micromechanical mechanisms do not vary with the origin of the salt, and the form is identical for all salts. As a result, this form can be used directly in determining the bound of the creep rates from a test or group of tests. However, because of the limitations of the steady state analysis, the approach for the analysis proposed in this work is significantly different. Both steady state and transient parameters are to be obtained from very limited data, perhaps a single creep curve. As a consequence, everything that is known about creep behavior in general, and salt creep behavior in particular, must be utilized. This means, in contrast to the steady state analysis procedure of the previous report, the transient analysis requires direct integration of the M-D equations themselves. The integration, however, is a simple, forward Euler integration method for the internal state parameter, ζ, evolutionary equation, and the creep strain, ε_c, equation. The fitting parameters in the process are the three material sensitive parameters already identified, the steady state creep rate through proportionality to A_2, the transient strain limit through K_0, and the rate of workhardening through α. In this manner, a complete fit to the experimental creep data can be obtained by trial and error variation of these three parameters.

The procedure was initiated by the selection of the parameters as obtained from the earlier steady state analysis method [Munson, 1998], together with the proper independent inputs for the stress and temperature of the test. Based on the results of this initial fit, and the relative steady state and transient contributions, as visualized in Figure 1, all of the structure factors, always in proportion to A_2, and the value of K_0 were adjusted. From the comparison of the integrated creep curves with the experimental data, an estimate was made of the required change in α to obtain the proper curvature. Subsequent adjustments of these three parameters were made, as necessary, until the fit was deemed adequate. For creep data obtained from multiple increments, each increment was integrated in succession using the appropriate conditions of stress and temperature. The accumulated values of both the internal state and the creep strain from the previous increment were carried forward to the next increment. The result was a complete fit to the data throughout all of the incremental changes in stress and temperature. Here, also, a trial and error iteration of the fit eventually led to acceptable simulation of the test data.

Even though the process is straightforward, a number of uncertainties can degrade the quality of the fit. These can originate from a number of sources. Perhaps the most critical uncertainty is the potential for the theoretical framework to be in error. In this instance, however, it is unlikely that any set of logical fits to the data could be obtained. For such an error to persist in the theory is normally quite unlikely.

The most probable sources of uncertainty and error in the analysis are characteristically more mundane, relating to the details of the testing and the analysis. These sources may, in part, be the result of undocumented experimental errors. They can also result from encountering data fundamentally out of the range of the model. While both of these

sources of uncertainties exist in the fits, the experimental errors lead to non-systematic discrepancies in the fitting, whereas the range problems tend to be systematic. An example of an experimental error is in the incorrect determination of the loading strain caused by slack or misalignment in the mechanical system or from insensitive initial zeroing of the gages. These errors can also be encountered during changes in stress and temperature during incremental testing. Perhaps the most difficult source of error is related to equipment hysteresis where material straining is masked by apparent progressive removal of mechanical slack from the system. Such experimental errors can lead to unusually large or small initial strain offsets and abnormal transient responses. When the analysis results are compared to the experimental data, some of these experimental difficulties may become evident. In fact, the analysis will be used to suggest where some possible experimental ambiguities exist.

An example of a range error is that which occurs when a given parameter is actually a function of an input condition, such as temperature, that has not been specifically evaluated for variations in that input condition. Such an error causes systematic deviation between experimental results and model prediction. Specific instances of range types of discrepancies were found during the analysis of the creep data.

4.0 DOMAL SALTS RESULTS

In two of the domal salt creep databases, test methods were used that could conventionally evaluate all of the important M-D parameters. In these cases, Weeks Island (WI) and Avery Island (AI) salts, transient analysis of the data is unnecessary. In all of the other cases, however, there were insufficient data to evaluate the parameters directly. These databases, Bryan Mound (BM), West Hackberry (WH), Bayou Choctaw (BC), Big Hill (BH), Moss Bluff (MB), and Jennings Dome (JD), may consist of standard creep tests terminated before steady state or of multiple increment tests. The database may contain the results from only one creep specimen or from several creep specimens. The specimens themselves may be from cores taken from different wells or from different locations in the same well. The tests are listed by the numbers assigned for the analysis and include all of the available domal salt databases except the extensive results for Avery Island, a database too large to be included here. Exact locations from which the specimens were obtained will always be clear from the identification nomenclature associated with the test number assigned during the analysis. The conditions of the individual tests, or increments of a test, are the stress, temperature, and duration and are specified in Table I. The identification nomenclature gives the salt dome, the well number, and the depth, in feet, of the core in the well from which the specimen was taken.

4.1 WEEKS ISLAND (WI) AND AVERY ISLAND (AI) SALTS

Because the creep databases for both the Weeks Island [Mellegard and Pfeifle, 1996; Munson and Ehgartner, 1997] and Avery Island [DeVries, 1988; Mellegard et al., 1983] domal salts are complete, there is no need to perform a transient analysis of the data. In these databases, a number of standard creep tests yield directly the values of the relevant parameters of steady state creep rate, transient strain limit, and initial value of the curvature. Even though these databases are still quite limited, there is no requirement to obtain the parameters through integration. For these two domal materials, the initial conventional parameter determinations as reported by Munson [1998] will be used. Some of these parameter value results for Weeks Island and Avery Island salts are repeated in Table II. However, for these two domal salts, one must refer to the original report for the complete set of parameter values.

Even though these two domal salts are not being subjected to transient analysis, they require some discussion within the concept of this report. While the parameter values determined may be quite precise, they are obtained from very restricted areas of the domes. Specimens were obtained for testing from a single borehole (BH3) for Weeks Island and from a single underground alcove mine location (164 m level) for Avery Island [Munson, 1998]. As a result, these databases are not a sampling of the overall dome. However, according to the results in Table II, it appears that the Weeks Island salt is slightly more creep resistant than the WIPP Baseline salt, but would still be considered as a soft salt. The parameters other than the steady state rates are essentially identical to those of the Baseline salt. The Avery Island salt is of equivalent creep resistance to the Weeks Island salt and would be considered as a soft salt. A smaller transient strain limit was found for Avery Island salt. Since both of these salts are

Table I. Creep Conditions and Data from Tests on Domal Salts.

Dome Specimen	Increment No.	Duration (Hrs)	Stress (MPa)	Temp. (°C)	Final Rate (10^{-10}/s)	Notes
WEEKS ISLAND						
WI 1	1	2352	20	25	27.5	[1]
WI 2	1	4104	15	25	9.73	
WI 3	1	3672	15	25	8.39	
	2	744	15	90	391.0	
WI 4	1	2136	10	25	0.665	
WEST HACKBERRY						
WH1	1	475	20.4	22	94.7	[2]
WH2	1	263	20.0	80(60?)	723.0	
WH3	1	262	20.0	22	119.0	
WH4	1	72	19.9	80(60?)	597.0	
WH5	1	148	20.8	60	596.0	[3]
	2	104	18.8	60	130.0	
	3	112	16.8	60	20.8	
	4	163	14.0	60	0.30	
	5	121	14.0	80	38.0	
WH6	1	287	13.6	60	88.0	
	2	193	16.8	60	248.0	
	3	118	16.7	80	659.0	
	4	146	17.0	60	163.0	
	5	101	20.2	60	619.0	
	6	167	16.7	60	275.0	
BIG HILL						
BH1	1	370	14.9	60	103.0	[4]
	2	70	15.0	80	402.4	
	3	934	15.1	60	137.8	
	4	243	17.9	60	364.0	
BH2	1	458	14.4	60	119.0	
	2	108	14.4	80	437.0	
	3	766	14.5	60	221.0	
	4	222	17.3	60	479.0	
BH3	1	409	15.1	60	142.0	
	2	120	15.1	70	271.0	
	3	166	15.1	60	132.3	
	4	286	17.9	60	363.0	
	5	51	17.9	70	834.0	
	6	149	17.9	60	446.0	

Table I (Cont.). Creep Conditions and Data from Tests on Domal Salts.

Dome Specimen	Increment No.	Duration (Hrs)	Stress (MPa)	Temp. (°C)	Final Rate (10^{-10}/s)	Notes
BAYOU CHOCTAW						
BC1	1	480	14.7	60	34.9	[3]
	2	313	14.7	80	81.6	
	3	44	12.8	80	8.0	
	4	268	14.8	80	66.0	
	5	66	12.7	80	4.6	
	6	175	14.7	80	55.0	
	7	305	14.8	60	11.3	
	8	2	17.1	60	?	
	9	266	14.8	60	6.8	
	10	24	17.0	60	37.0	
	11	145	14.9	60	4.7	
	12	407	17.1	60	37.0	
	13	91	14.8	60	1.0	
BRYAN MOUND						
BM1	1	410	10.1	60	2.52	[5]
	2	332	21.6	60	22.0	
BM2	1	457	20.8	22(60?)	9.0	
BM3	1	280	20.6	60(22?)	27.5	
BM4	1	264	20.6	22	12.4	
BM5	1	143	20.6	22	92.0	[3]
	2	67	21.1	22	41.0	
	3	120	20.5	22	27.0	
	4	118	19.9	60	87.0	
	5	99	19.9	100	969.0	
	6	101	20.1	60	49.0	
BM6	1	74	16.0	59	28.1	
	2	42	16.2	59	27.8	
	3	214	22.6	59	66.9	
BM7	1	313	20.9	22	21.2	
	2	311	21.0	60	55.9	
BM8	1	700	14.2	60.4	16.0	
	2	139	21.7	60.2	110.0	
BM9	1	361	14.0	59.7	11.0	
	2	74	14.1	79.8	26.0	
	3	94	14.4	79.8	27.0	
	4	148	14.4	59.8	6.0	
	5	337	15.4	59.8	7.4	

Table I (Cont.). Creep Conditions and Data from Tests on Domal Salts.

Dome / Specimen	Increment No.	Duration (Hrs)	Stress (MPa)	Temp. (°C)	Final Rate (10^{-10}/s)	Notes
BRYAN MOUND						
BM9(Cont.)	6	258	15.3	80	24.0	
	7	246	15.3	59.6	4.7	
	8	356	20.6	59.6	43.0	
	9	364	20.5	80	91.4	
	10	307	20.5	59.4	22.0	
	11	269(369)	22.1	59.4	32.8	
	12	483(383)	24.5	59.4	96.0	
	13	137	24.5	80	365.0	
	14	328	24.5	33.5	14.0	
BM10	1	163	17.3	40	108.5	
	2	144	17.2	60	232.0	
	3	50	17.1	80	850.0	
	4	97	17.2	59.8	128.0	
	5	404	17.2	39.8	29.6	
	6	147	19.7	40	85.0	
	7	95	19.6	59.8	328.0	
	8	193	19.6	40	56.3	
	9	53	19.5	79.6	1258.0	
	10	114	19.6	59.8	331.6	
JENNINGS DOME						
JD1	1	330	17.4	39.8	14.2	[6]
	2	108	16.3	59.7	9.4	
	3	485	17.3	59.7	22.0	
	4	594	19.7	59.7	34.8	
	5	269	19.7	39.7	4.4	
MOSS BLUFF						
MB1	1	341	16.0	40.1	74.2	[7]
	2	426	6.1	58.9	118.0	
	3	676	19.5	58.9	214.0	
	4	241	19.5	39.7	52.1	

Notes: [1] Mellegard and Pfeifle, 1996. [2] Wawersik et al., 1980a. [3] Wawersik and Zeuch, 1984. [4] Wawersik, 1985. [5] Wawersik et al., 1980b. [6] Wawersik and Zimmerer, 1994. [7] Wawersik, 1992.

associated with conventional mines, it is not possible to establish equivalent cavern closure creep rates. Regardless of the differences between the Weeks Island, Avery Island, and the WIPP Baseline parameters, they appear to be very similar in their behavior. This is especially true of the Weeks Island and WIPP Baseline salts.

Geological studies of the Weeks Island dome have been based on examination of the underground structures exposed by mining and surface evidence suggestive of faulting [Ortiz, 1980]. A general description of the dome geology [Neal et al., 1993a] suggests the possibility of several salt zones (which they called spines) separated by features of higher impurity concentrations. The concentrations were postulated to arise through induction of impurities into zones of shear during the mechanical displacement of adjacent salt masses.

Kupfer [1963], primarily on the basis of underground structures exposed by mining, has suggested a rather complicated geology for the Avery Island dome. The postulated structure consists of two distinct zones of salt separated by an extensive zone of coarse salt.

4.2 BRYAN MOUND (BM) SALT

Munson [1998], on the basis of the steady state analysis, categorized this dome as being composed of "hard" salt. However, when the comparison of the CAVEMAN volume creep characteristics [Linn, 1997] were taken into account, this categorization seemed too simplified. Some caverns were obviously much softer than the steady state analysis suggested. This discrepancy drove the need to analyze the data in detail through the more revealing transient analysis process.

Based on surrounding strata, surface, and cap rock expressions of possible faults [Neal et al., 1994] postulated a geologic structure for the dome. As a result of the study, two "anomalous" zones are proposed, based on a collection of several features, such as fault traces, impurities, etc. One runs from northwest to southeast, the other from northeast to southwest, nearly at right angles to each other with the intersection displaced slightly off center to the northeast. As supported by petrographic analysis of salt core, these features appear to extend in depth into the dome to define possible spines. Recently, Looff and Looff [1999] have used isopach analysis and interpretation of faulting in the surrounding strata to expand and modify the locations of the postulated shear zones. The fault locations differ in detail from those suggested by Neal et al. [1994].

The database for Bryan Mound consists of ten tests, involving four different wells and up to as many as five separate coring locations in a given well. The earlier data [Wawersik et al., 1980b] was in the form of standard creep tests involving material from two different wells, 107A and 107B, of the same cavern. Actually, one of these tests was a two-increment test where only the stress, temperature, and time conditions of the first stage were reported. While the increment could be calculated, comparison to the workhardening data was not possible. The transient analysis of these tests certainly illustrates the potential difficulties faced in interpretation of experimental data. In fact, this was only the beginning of a number of discrepancies noted between reported results and analysis.

Table II. Transient Analysis M-D Model Parameters for Domal Salts.

Specimen	A_2(x10^{12}/s) #	Factor	K_0(x10^5/s)	Factor	α(T(°C))	Factor	Closure (%/yr.)
BASELINE	9.672	1.00	6.275	1.00	-17.35(25)	1.00	WIPP Clean Salt
AVERY ISLAND DOME (Conventional Analysis, Parameters from Munson [1998])							
	6.869	0.71	1.342	0.21	-13.20(25)	0.76	?
WEEKS ISLAND DOME (Conventional Analysis, Parameters from Munson [1998])							
	5.706	0.59	6.275	1.00	-17.35(25)	1.00	?
BRYAN MOUND DOME							
				Cavern 113			
BM10 113-4225	**11.32**	1.17	**4.393**	0.70	**-13.37**(60)	0.54	0.12 (Soft)
					-9.37(80)	0.42	
				Cavern 107			
BM5 107B-3324	**2.647**	0.27	**3.640**	0.58	**-13.37**(22)	0.77	0.02 (Hard)
					-9.37(60)	0.54	
					-6.37(100)	0.37	
BM9 107C-2508	**0.2965**	0.03	**4.050**	0.65	**-13.37**(30)	0.77	(Very Hard)
					-9.37(60)	0.54	
					-7.37(80)	0.42	
BM8 107C-2506	**0.2965**	0.03	**3.640**	0.58	**-9.37**(60)	0.54	(Very Hard)
BM7 107C-2516	**0.2965**	0.03	**2.904**	0.46	**-13.37**(22)	0.77	(Very Hard)
					-9.37(60)	0.54	
BM6 107C-2517	**0.2965**	0.03	**2.904**	0.46	**-9.37**(60)	0.54	(Very Hard)
BM4 107C-2504	**0.2609**	0.03	**1.335**	0.21	**-13.37**(22)	0.77	(Very Hard)
BM3 107C-2507	**0.2609**	0.03	**1.335**	0.21	**-9.37**(60?)*	0.54	(Very Hard)
BM2 107A-3965	**0.2609**	0.03	**1.335**	0.21	**-13.37**(22?)*	0.77	(Very Hard)
BM1 107A-3966	**0.2609**	0.03	**1.335**	0.21	**-9.37**(60)	0.54	(Very Hard)
WEST HACKBERRY DOME							
				Cavern 6C			
WH1 6C-2243	**11.32**	1.17	**9.777**	1.56	**-17.37**(22)	1.00	(Very Soft)
WH3 6C-2225	**11.32**	1.17	**9.777**	1.56	**-17.37**(22)	1.00	(Very Soft)
WH2 6C-2201	**11.32**	1.17	**9.777**	1.56	**-17.37**(80?)*	1.00	(Very Soft)
WH4 6C-2196	**11.32**	1.17	**9.777**	1.56	**-17.37**(80?)*	1.00	(Very Soft)
				Cavern 108			
WH5 108-2267	**11.32**	1.17	**8.512**	1.36	**-13.37**(60)	0.77	0.145 (V. Soft)
			6.275**	1.00	**-9.37**(80)	0.54	
WH6 108-3652	**11.32**	1.17	**8.512**	1.36	**-13.37**(60)	0.77	0.145 (V. Soft)
			6.275**	1.00	**-9.37**(80)	0.54	

Table II. (Cont.). Transient Analysis M-D Model Parameters for Domal Salts.

Specimen	A_2(x10^{12}/s) # --------Factor	K_0(x10^5/s) --------Factor	α(T(°C)) ----------Factor	Closure (%/yr.)
BIG HILL				
		Cavern 106		
BH1 106B-5465	**11.32** 1.17	**6.275)** 1.00	**-13.37**(60) 0.77	0.09 (Soft)
			-9.37(80) 0.54	
		Cavern 108		
BH2 108B-2517	**15.85** 1.64	**8.512** 1.36	**-13.73**(60) 0.77	0.15 (Very Soft)
			-9.37(80) 0.54	
BH3 108B-3516	**15.85** 1.64	**8.512** 1.36	**-13.73**(60) 0.77	" (Very Soft)
BAYOU CHOWTAW				
		Cavern 19A		
BC1 19A-2577	**2.250** 0.23	**6.275** 1.00	**-13.73**(60) 0.77	0.06 (Hard)
			-9.37(80) 0.54	
MOSS BLUFF				
		Well MB		
MB1 MB2-3349	**6.770** 0.70	**8.964** 1.43	**-13.73**(60) 0.77	(Soft)
JENNINGS DOME				
		Well LA1		
JD1 LA1-3927	**1.222** 0.13	**1.308** 0.21	**-13.73**(60) 0.77	(Hard)

The quoted factor is just the ratio of the domal salt material A_2 parameter value to that of the WIPP clean salt baseline value. In order to form a complete set of parameters for a material this factor can be used to generate the remaining A and B values through multiplication of the corresponding Baseline steady state parameters.

* Appears to be some uncertainty in the reported values.

**These are very high stress increments, perhaps causing an increase in K_0.

Analysis began by using the steady state creep analysis parameter values as input to the integration process. Trial and error adjustment of the three fitting parameters finally produced the fits shown in Figures 3 and 4. In Figure 3 the calculated fit to BM1 appears extremely good; however, the fit to BM3 has some obvious problems (as well as a non-obvious problem). In this case, an acceptable fit to the calculated curve is obtained by a uniform vertical displacement of the BM3 data. While not very pleasing, uncertainty in the initial, or zero, strain value in experimental data can be a well-known occurrence in creep testing. As a consequence, we will suggest that the BM3 data have a zero strain

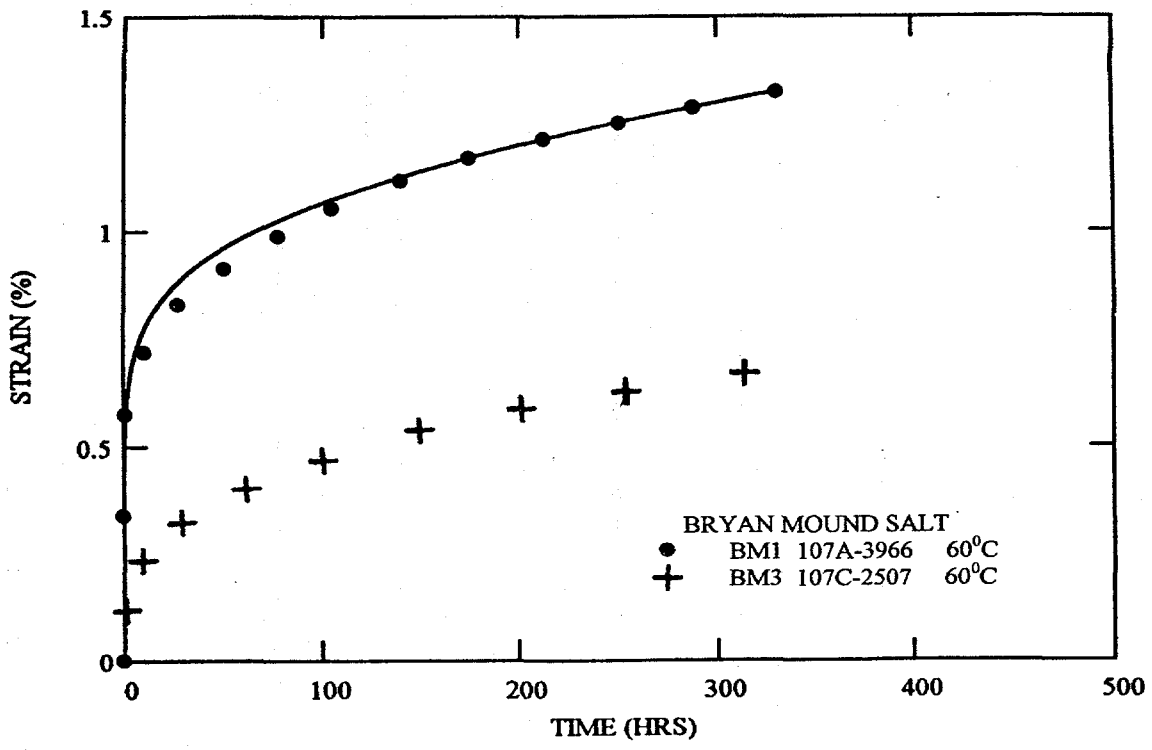

Figure 3. Calculated Fit (Solid Line) to Bryan Mound BM1 and BM 3 Data.

discrepancy. Unfortunately, even then, the agreement depends upon assuming that the temperature of the BM3 test was 60°C rather than the reported value of 22°C. Without changing the parameter values used in BM1 (107A) and BM3 (107C), the calculated fits for BM2 and BM4 were made. In Figure 4, the calculated fit to BM2 (107A) again appears to be very good, especially considering the same parameter values were used. Obviously, the fit to BM4 (107C) has some discrepancies. If the BM4 data are examined carefully, the data initially follow the fit and BM2 data very closely; but at about 10 hours, the BM4 data are displaced sharply upward. Inexplicably, this type of machine or instrument related displacement can occur and can obscure the material related response. Thereafter, the creep rate decreases markedly and erratically until it eventually becomes the same as the calculated fit and the BM2 data. It appears that a non-creep-related offset in strain occurred, followed by hysteresis caused by the over shoot in strain. What appears to happen is that the hysteresis eventually gives away to normal, creep related strain behavior. However, the offset is retained. BM2 has a similar problem to BM3 in that the fit shown is possible only if the test temperature is assumed to be 22°C rather than 60°C, as initially reported. While there is no independent information suggesting the temperatures of BM2 and BM3 were transposed when reported, it would be virtually impossible to obtain a rational fit to these data as initially reported. It also appears logical that the 107A specimens would be tested at two temperatures, as would the 107C specimens, rather than duplicating the test conditions on specimens from the same wells. Consequently, the risk of transposing temperatures as necessary to obtain the best fits is considered acceptable. Parameters obtained from the fits of BM1, BM3, BM2, and BM4 with this assumption are shown in Table I.

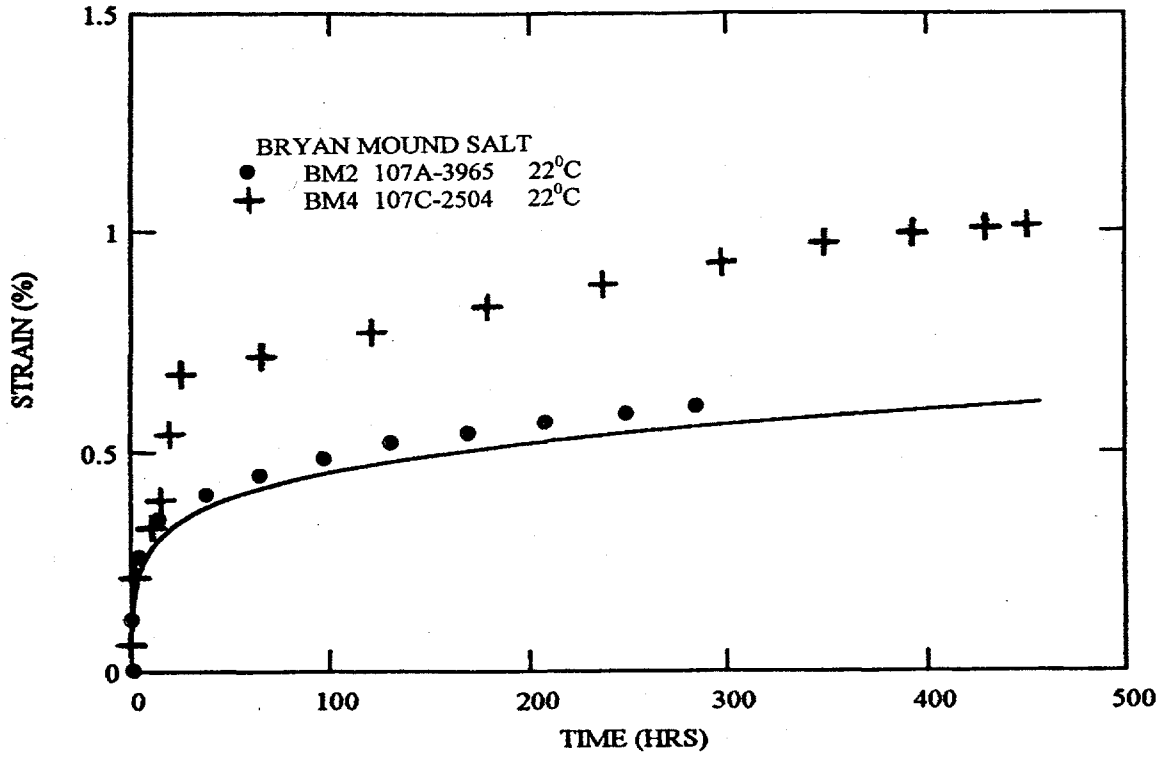

Figure 4. Calculated Fit (Solid Line) to Bryan Mound BM2 and BM4 Data.

These results also indicate the type of range error mentioned previously. In very early data analysis of WIPP salt, Munson and Dawson [1982] had shown that K_0 is a function of temperature and this was eventually incorporated into the model [Munson et al., 1989]. However, there was no specific indication in these early results that Δ was influenced by temperature because only one temperature level was analyzed, so no similar study of α was made. In the current transient analysis, the temperature range of the experimental data is greater, and the parameter sensitivity is apparent. Even though there is no provision in the M-D model for the temperature dependence of the α parameter, better fits are obtained here when this parameter changes value systematically with test temperature. As α decreases, the magnitude of Δ also decreases, and the curvature (workhardening rate) increases. The velocity of a free dislocation velocity in a virgin material is thought to be constant with temperature; however, the dislocation controlled steady state creep rate is not. Since Δ is just the logarithm of the ratio between these two quantities, α would appear to diminish with temperature.

In a later study [Wawersik and Zeuch, 1984], additional specimens of Bryan Mound salt were tested in incremental tests. The analysis comparisons are shown in Figures 5 through 8 for tests BM6, BM7, BM8, and BM9, all on material taken from Well 107C. In these multiple increment tests, while the steady state creep rate remained unchanged from the earlier analysis results, it was necessary to increase the transient strain limit. In these results a continuation of the fitting difficulties is observed. BM6 is a three-increment test, while BM7 and BM8 are two-increment tests. In these tests, some individual increments appear to be offset from the calculated curves. Without major changes in the parameters

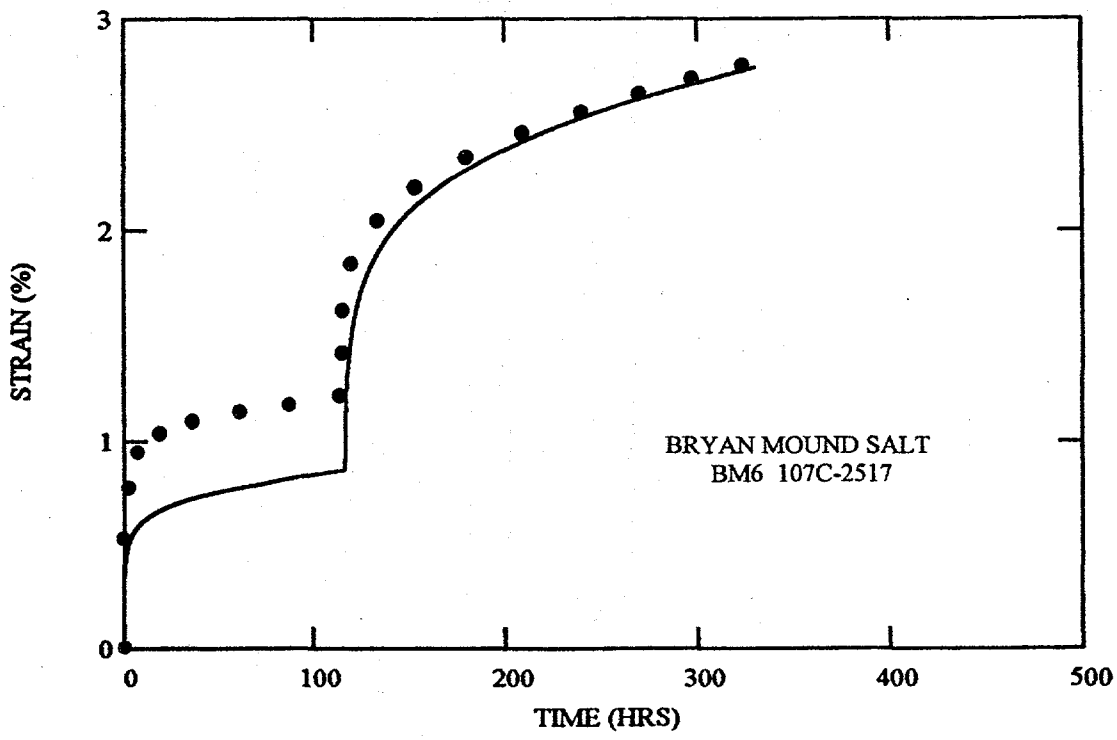

Figure 5. Calculated Fit (Solid Line) to Bryan Mound BM6 Data.

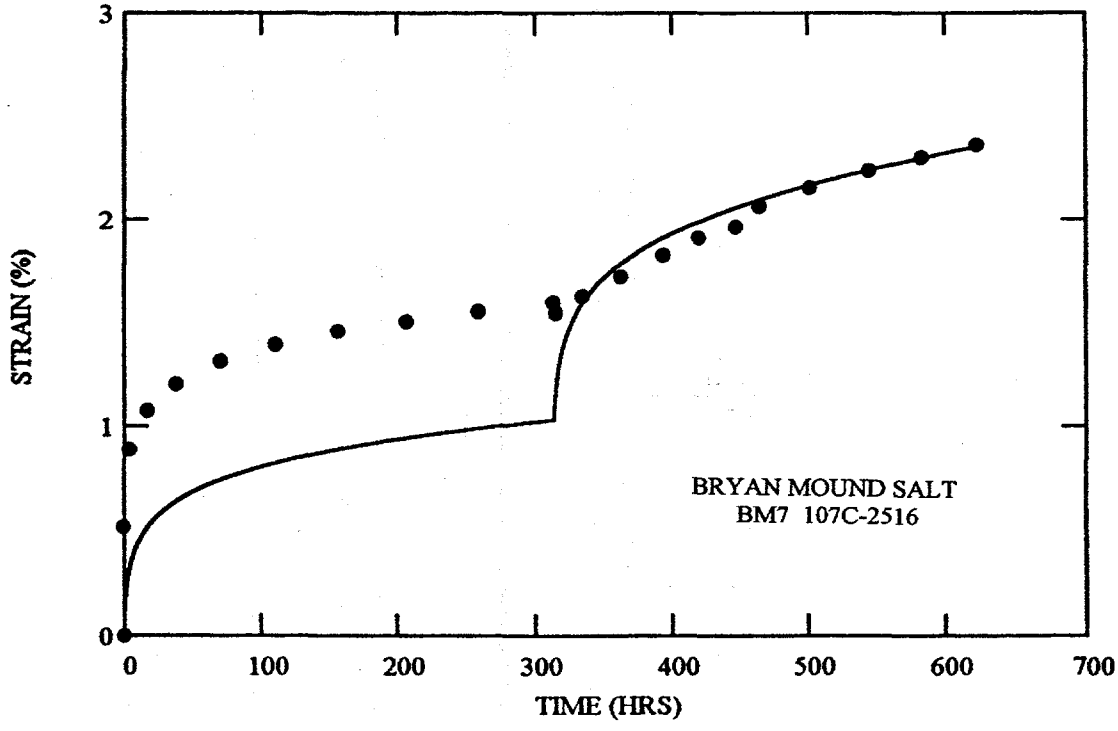

Figure 6. Calculated Fit (Solid Line) to Bryan Mound BM7 Data.

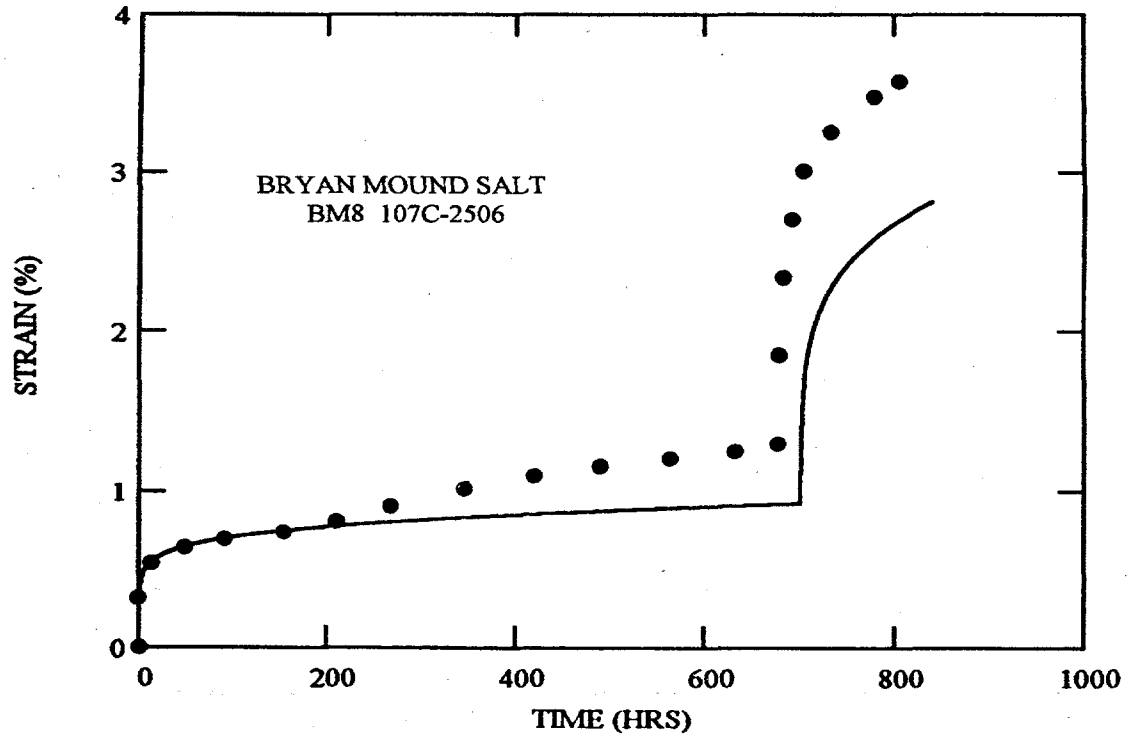

Figure 7. Calculated Fit (Solid Line) to Bryan Mound BM8 Data.

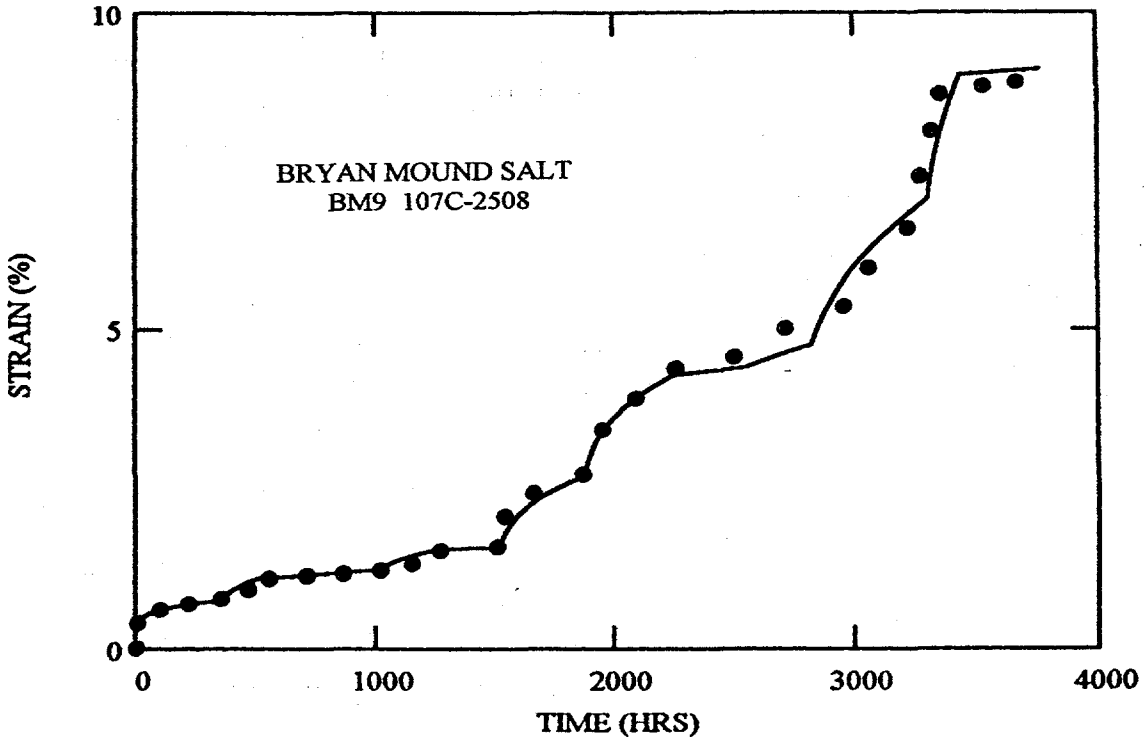

Figure 8. Calculated Fit (Solid Line) to Bryan Mound BM9 Data.

within one test, the analysis cannot fit all aspects of these tests. In the case of BM6, again without any independent proof, it appears that individual increments fit the shape and the strain rates of a given increment calculation, provided they can be displaced vertically in strain. In the case of BM7, the second increment has the appearance of hysteresis. In the case of BM8, the calculation and experiment are initially in good agreement, only to give way to a slow, abnormal, increase in creep strain. This vertical offset apparently continues throughout the final increment of the test. In the end, a set of parameters was obtained that gave the best "shape" regardless of the vertical offsets necessary to fit a given increment. As given in Table II, the transient strain limit is somewhat greater to obtain the fits in tests BM6 through BM8 than that required for the first four tests, BM1 through BM4.

In test BM9, on core also taken from Well 107C, there were 14 increments. Even though it is somewhat difficult to tell, most of the increments are well matched to the analysis calculation. There is some discrepancy between the calculation for the eighth and the ninth increments. A discrepancy was found in the listed and the graphical ending and beginning times between the increments. This discrepancy was not noticed before the calculation and, consequently, the discrepancy appears in the lack of fit in Figure 8 for these same increments. However, in general, the analysis results based on the integration seem very accurate. Here, a slight further increase in the transient strain limit, as given in Table II, was the only change required in the parameters.

At this point, the cores from Bryan Mound Wells 107A and 107C all correspond to hard salt, with about the same creep resistance. The only variation is the rather modest change in the transient strain limits.

There are only two Bryan Mound creep tests remaining to be discussed, BM5 and BM10. The core for these two specimens came from wells distinct from those discussed to this point. BM5 is from Well 107B and, as shown in Figure 9, is a six-increment test. The first three increments are under nearly identical conditions of stress and temperature, with only a change in confining pressure from 6.9 MPa to 13.8 MPa between increment one and two, at about 150 hours. Because the dislocation mechanism that controls the creep process is insensitive to pressure [Chan et al., 1998], there should be no affect on the creep response. However, the experimental results show a vertical shift at the time of pressure change. It is suspected that this vertical shift is the result of a machine-induced offset at the time of the adjustments in pressure. But, before and after this perturbation, the creep rates remain almost unchanged, as expected. Again in this test, the initial portion of the data appears offset from the calculation, an offset that is removed in the fourth increment in what appears to be recovery through hysteresis. As the results in Table II indicate, BM5 was found to have a higher steady state creep rate, about a factor of 10, from those tests previously presented. This suggests that the salt of Well 107B is not as creep resistant, at least from this depth, as the salt from the other two wells of the cavern. These wells were separated laterally by 15 to 35 m. An increase in the transient strain limit was also apparent. Regardless of these differences in the creep characteristics of the salt specimens from the three wells of this cavern, the salts would all still be considered as hard or creep resistant.

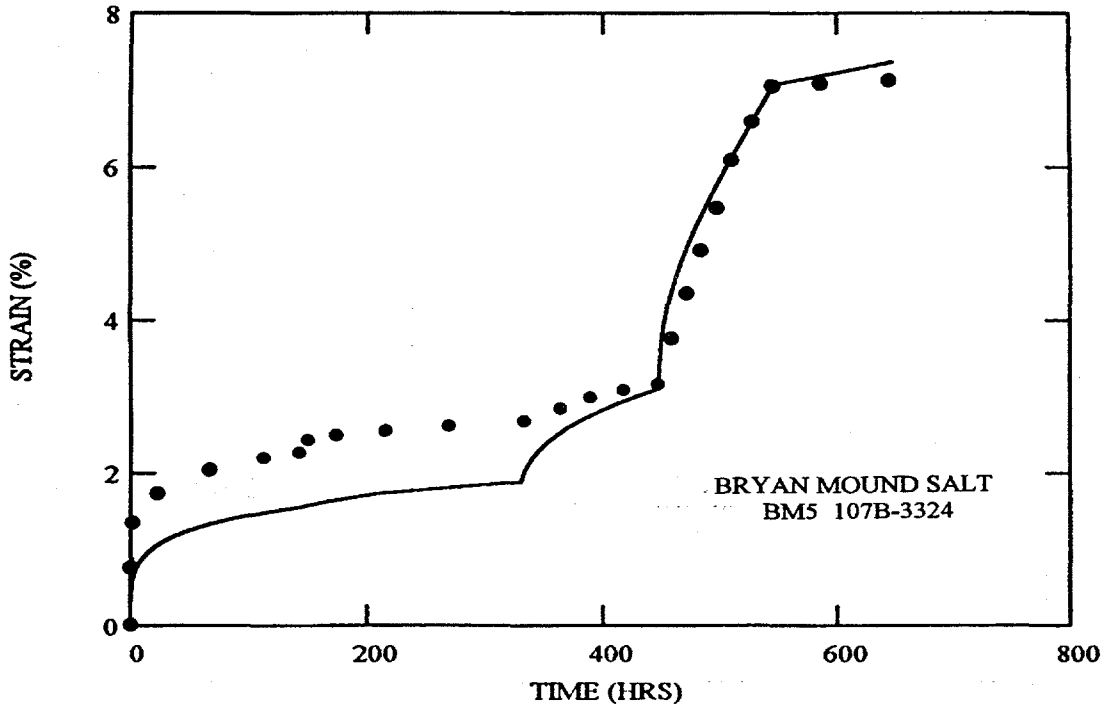

Figure 9. Calculated Fit (Solid Line) to Bryan Mound BM5 Data.

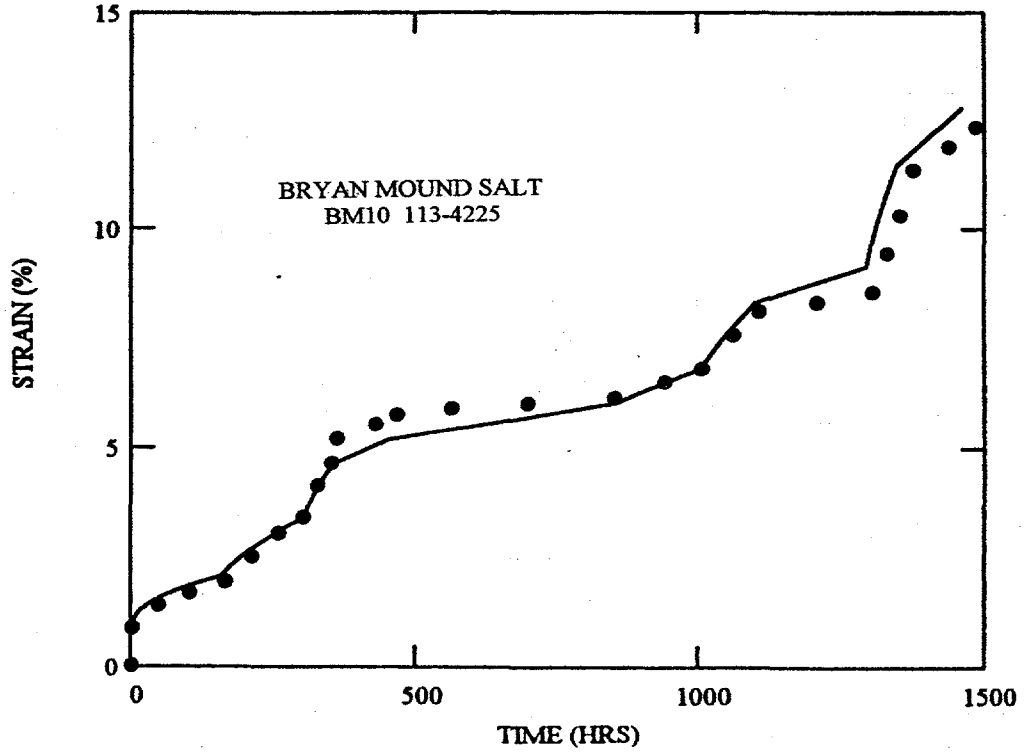

Figure 10. Calculated Fit (Solid Line) to Bryan Mound BM10 Data.

Test BM10 was on specimen material taken from Well 113. This single, ten-increment test was well simulated by the calculation, as shown in Figure 10. A relatively minor offset occurs between the third and fourth increments and there is disagreement in the rates of the eighth (stress drop) increment. The parameters necessary to obtain this fit are given in Table II. It is clear that this BM113 salt material is very "soft" and has much less creep resistance than the material from BM107. This difference is reflected in the relative values of the CAVEMAN volume loss creep rates, as also given in Table II.

4.3 WEST HACKBERRY (WH) SALT

The creep database for the West Hackberry SPR facility [Wawersik and Zeuch, 1984; Wawersik et al., 1980a] consists of six separate specimens from two different wells, 6C and 108. In Phase I of the SPR Project, the initial caverns were available commercial caverns purchased for the rapid implementation of the oil reserve program. After the initial phase, special caverns were designed, solution mined, and placed in service during Phases II and III of the Project according to the SPR Project specifications. These purpose-built or -constructed caverns were all very similar in geometry, amount of overburden, and their depth in the salt. Their construction was very carefully controlled. The 6C cavern was an existing commercial cavern purchased by the SPR Project in Phase I, as such the construction was not well controlled and it differs markedly in configuration from the Phase II and III caverns. Cavern 108 was purpose-constructed by the SPR Project and is a well-configured cylindrical cavern with nominal dimensions similar to all of the other purpose-constructed SPR caverns. The creep results from the West Hackberry creep tests are extremely consistent, much more so than for the Bryan Mound data discussed above.

Geologically, the West Hackberry salt dome is thought to contain at least two postulated anomalous zones, which Magorian et al. [1991] described as possible shear zones. The shear zones are defined by increased amounts of anhydrite. There are many minor surface defined faults that may or may not extend into the salt. One of the probable shear zones extends from the middle of the west edge toward the south-southeast at about 15°. The other probable shear zone extends from the middle of the north edge across the dome to the south edge at an angle of about 15° west. Magorian et al. [1991] suggested that this north-south trending anomalous feature separated two probable displacement spines.

The four tests on the Well 6C materials were all conventional creep tests, terminated prior to attaining steady state. The two tests on Well 108 materials were multiple increment tests, involving two separate specimens. The calculated integrated fits are compared to the experimental results in Figures 11 through 14. Analysis of the creep database is very straightforward (almost) for the first four tests. WH1 and WH3 data at 22°C are compared to the integration using the best-fit parameters in Figure 11. The creep data are consistent with each other, and the fits are almost exact. Using these same parameters determined at 22°C, the tests at the higher temperature were simulated. Interestingly, the calculated fits for these higher temperature tests did not match the data when the reported temperature of these tests was used. In fact, a logical set of parameters could not be developed for these two tests. When the reported temperature was used, the form of the prediction appeared to

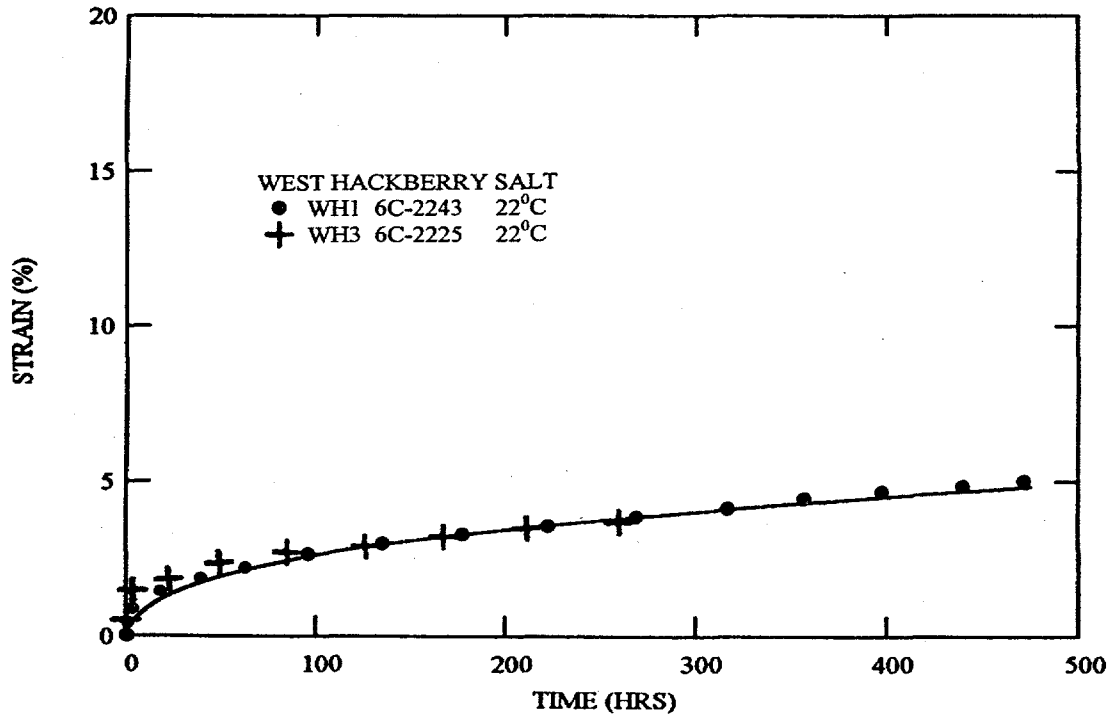

Figure 11. Calculated Fit (Solid Line) to West Hackberry WH1 and WH3 Data.

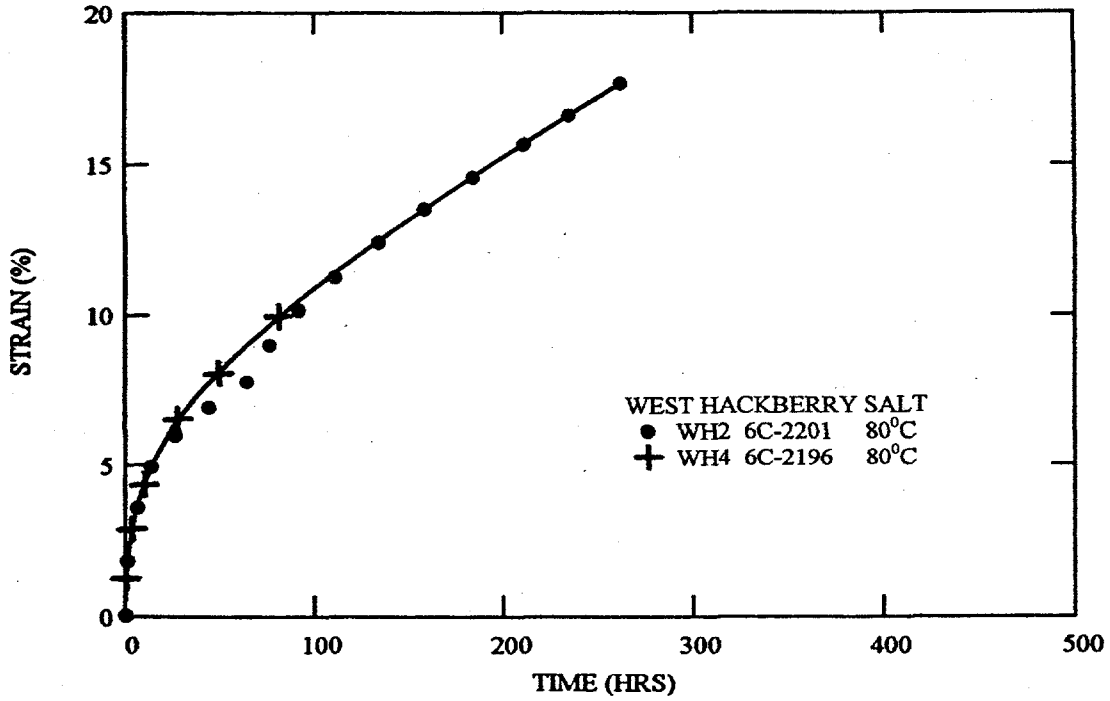

Figure 12. Calculated Fit (Solid Line) to West Hackberry WH2 and WH4 Data.

under predict the data by a simple multiplication ratio. It is not possible with changes in either the steady state rate or the transient strain limit to cause such a simple multiplication correction, whereas the characteristic temperature dependence could. Subsequently, when the temperature of the tests was assumed to be 80°C, excellent simulations were obtained. The fact that a simple increase in temperature from 60° to 80°C produced such a good fit certainly points to a possible reporting error. However, the reported conditions were internally very consistent and it is not actually known that they are indeed incorrect. While it cannot be known with certainty that the reported temperatures were in error, the fitting procedure suggests this as a distinct and logical possibility. The predicted results are shown in Figure 12. On this basis, the fitting parameters are given in Table II.

Test WH5, as shown in Figure 13, consists of five increments, primarily descending through successive stress drops from the initial stress condition. Integration to obtain a good fit was possible using the same steady state rates as in the first four tests, but with a slightly smaller value of K_0. The calculated response to all of the stress drops of this experiment is interesting. Although the match to the stress drops is probably adequate, the discrepancy is such that calculation over predicts the subsequent strain rates. In fact, if all of the previously fitted stress drop increments are examined, the calculations consistently over predict the creep rate after the stress drop. As initially noted, the recovery parameter, δ, is not taken as a fitting parameter in this analysis, and no adjustment was made. Regardless, considering the small magnitude of the discrepancies, the current analysis basis is probably adequate.

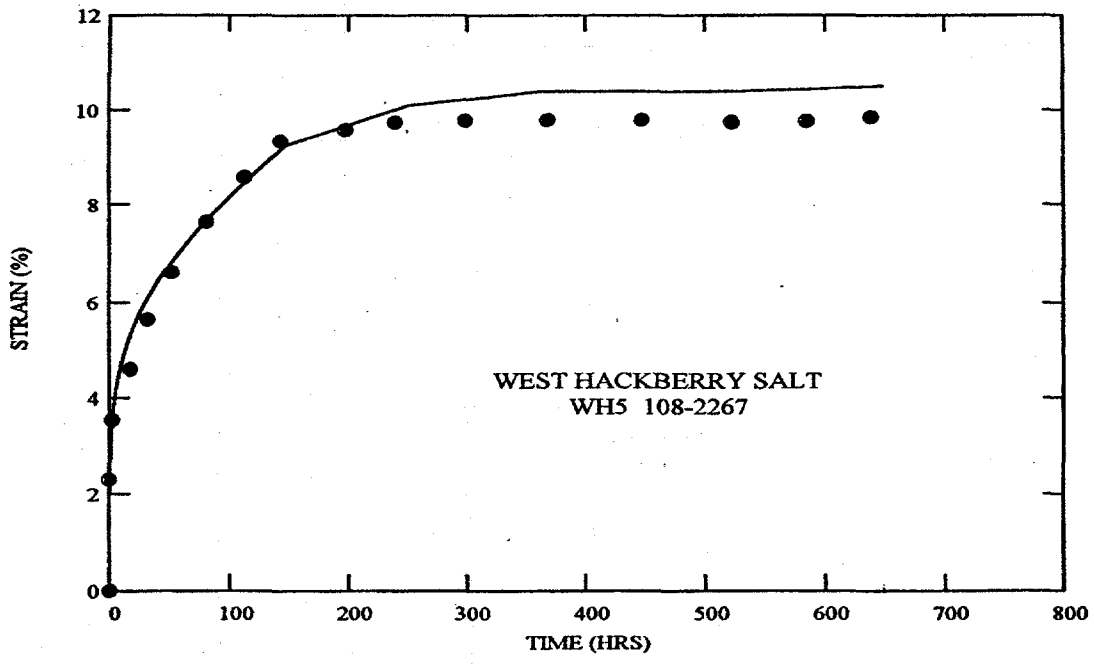

Figure 13. Calculated Fit (Solid Line) to West Hackberry WH5 Data.

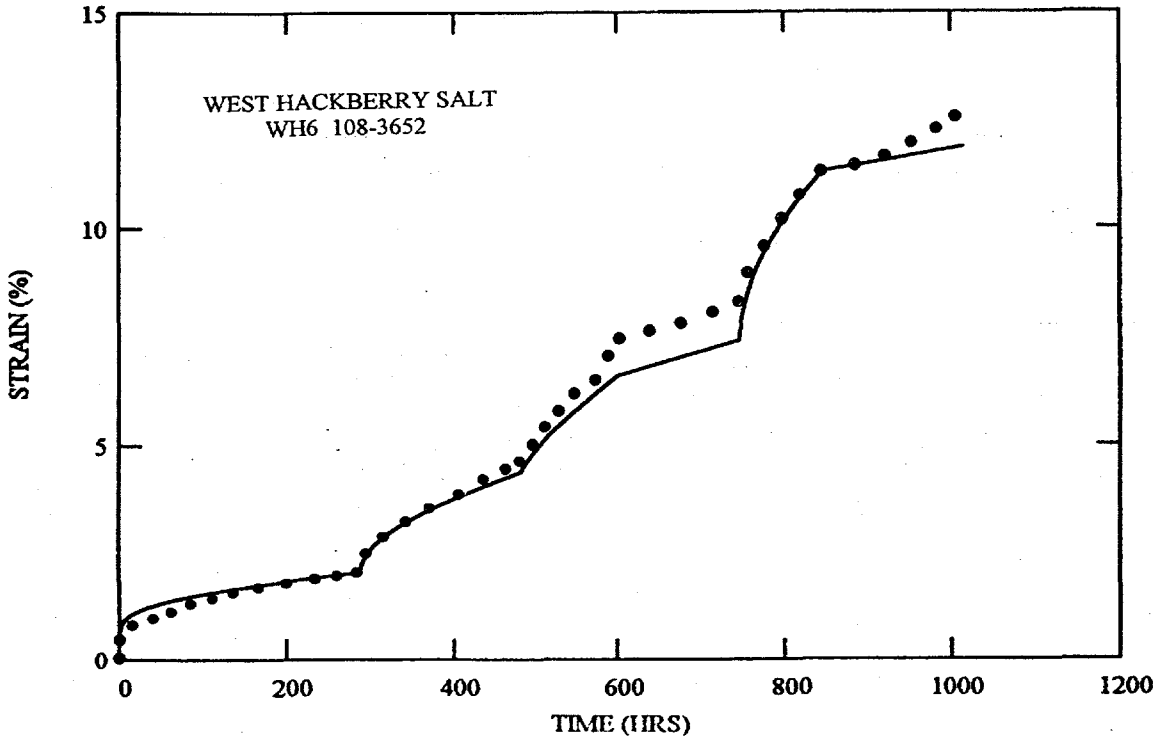

Figure 14. Calculated Fit (Solid Line) to West Hackberry WH6 Data.

Test WH6, as shown in Figure 14, consists of six increments. Again using the same steady state parameters and the same K_0 as for WH5, the integration gives quite an acceptable simulation of the experimental data. A slight upward offset is noted between the third and fourth increments, which is apparently eliminated in the fifth increment. Although the behavior may never be known exactly, this is possibly an apparatus offset strain at the time of the stress change that was taken out by hysteresis after the following stress change. The fitting parameters are given in Table II.

All fits to the creep data from the four specimens obtained from two wells at West Hackberry were quite reasonable, with consistency obtained in the fitting parameters. It is clear that the West Hackberry salt, at least on the basis of the four specimens from the two wells tested, is a very soft salt. This is directly confirmed by the comparable CAVEMAN measures of cavern creep closure.

4.4 BIG HILL (BH) SALT

For the Big Hill SPR facility, geomechanical test data [Wawersik, 1985] from two different wells are available, with multiple tests from the specimens of one of the wells. Test BH1 is a four-increment test from Well 106B. Tests BH2 and BH3 are four-increment and six-increment tests, respectively, from Well 108B. The best fit to BH1 is shown in Figure 15. Although the fit is acceptable, there are indications of a growing discrepancy at high strains and long times where the data almost suggest the development of a tertiary creep behavior. In fact, this same general response is found in BH2 and BH3. Fits to these two sets of data are shown in Figures 16 and 17. The late time discrepancy in

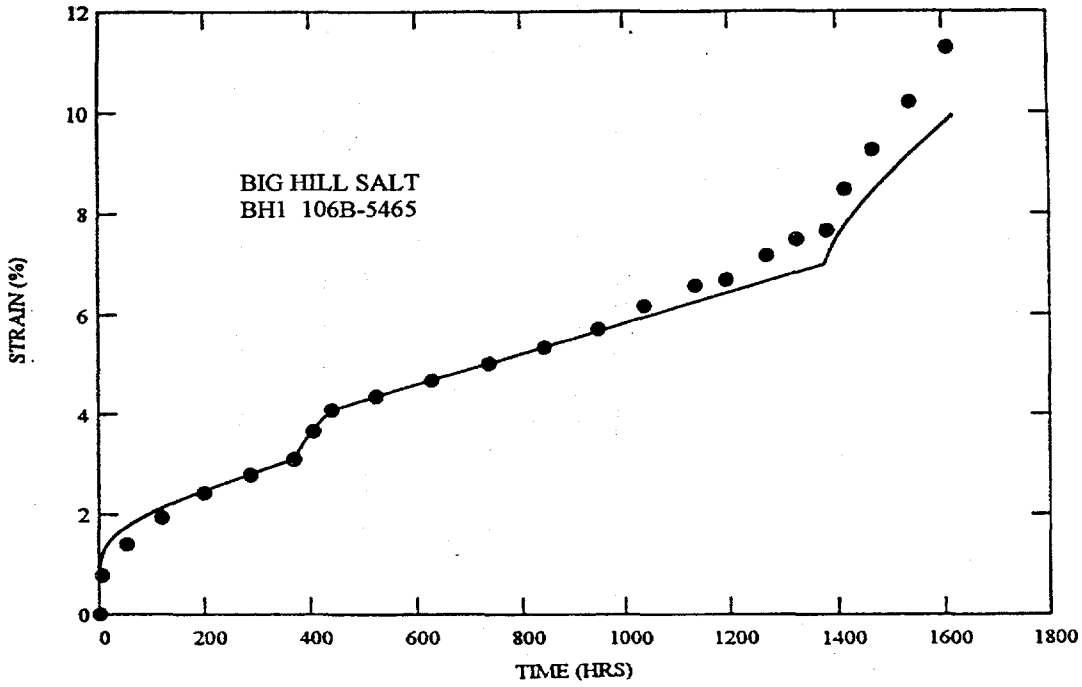

Figure 15. Calculated Fit (Solid Line) to Big Hill BH1 Data.

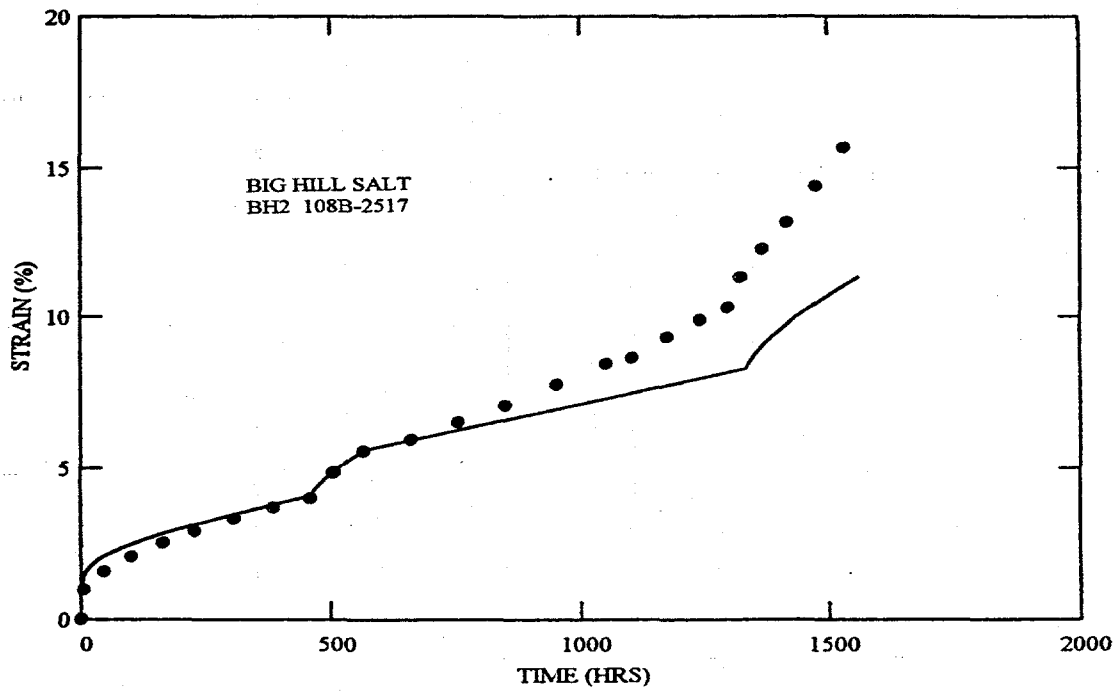

Figure 16. Calculated Fit (Solid Line) to Big Hill BH2 Data.

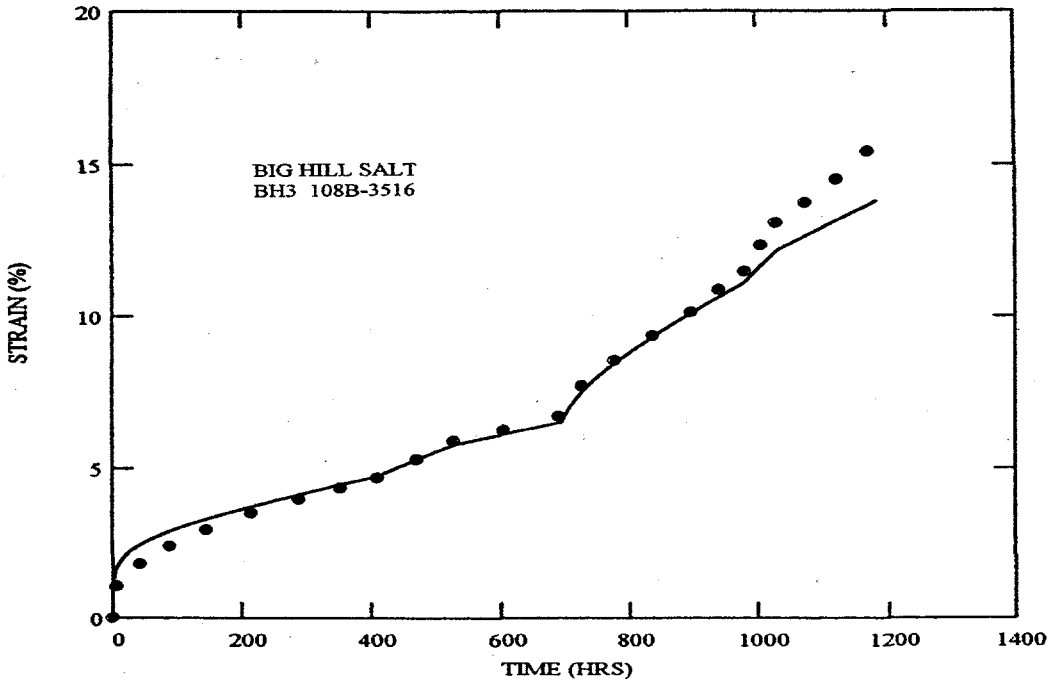

Figure 17. Calculated Fit (Solid Line) to Big Hill BH3 Data.

BH2 is especially pronounced. Based on what is known about the complete suppression of fracture in pure salt for confining pressures above 5.5 MPa [Chan et al., 1998], the 13.8 MPa confining pressure on these tests certainly should prevent the development of tertiary creep. In any event, the form of the experimental curves is clearly different than one would expect under these pressure conditions. A major exception could occur if the Big Hill material contained significant impurities, which tend to decrease the affect of confining pressure [Chan et al., 1996] so that tertiary creep can occur at higher confining pressures. However, there is no indication of the salt of Big Hill having impurity contents much different than the other SPR dome sites. Parameter values obtained from the fits for these tests are given in Table I and indicate the Big Hill salt is quite soft, with little creep resistance. The CAVEMAN results for the volume creep closure certainly support this contention.

Geologically, Neal et al. [1993a] proposed a probable anomalous zone or shear zone traversing the dome in the north-south direction. Apparently, numerous surface faults exist in the cap rock, some of which are thought to extend into the salt dome. Significant fault displacements exist above the proposed shear zone. It should be noted, moreover, that Big Hill caverns during construction were considerable as very "gassy."

4.5 BAYOU CHOCTAW (BC) SALT

Only a single specimen was tested from material at the SPR Bayou Choctaw dome facility [Wawersik and Zeuch, 1984]. Test BC1 was a 13-increment test on a specimen taken from core of Well 19A. Cavern 19 was a commercial cavern purchased for use by the

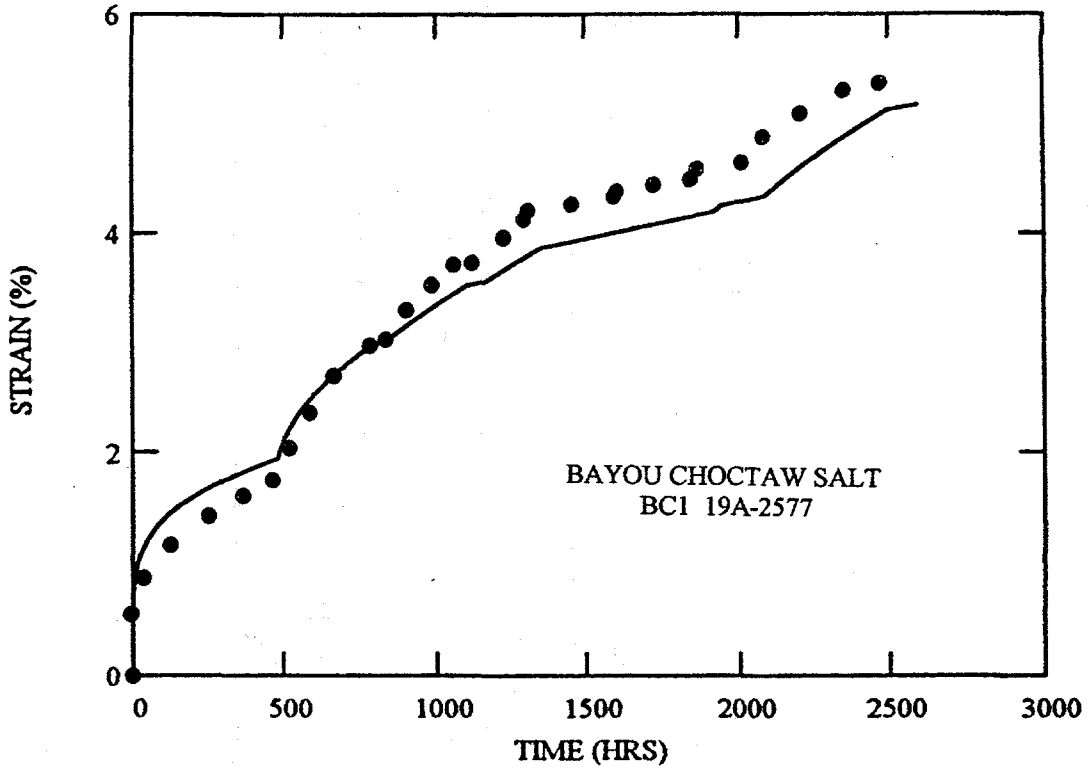

Figure 18. Calculated Fit (Solid Line) to Bayou Choctaw BC1 Data.

SPR Program. Because of its commercial beginnings, it has an irregular geometry, considerably different than the cylindrical symmetry of the SPR purpose-constructed caverns. Because of the large number of increments, the integration process was difficult for these data due to computer capacity limitations. The initial under prediction becomes an over prediction in the later increments. The discrepancy does not appear to result from offsets. While a somewhat larger steady state creep rate might seem appropriate, it is not certain any adjustment would be satisfactory. Thus, although there remain some discrepancies, the parameters used for the calculated fit given in Figure 18 appear to be adequate. The salt of the Bayou Choctaw dome is seen to be relatively creep resistant, although not as resistant as the hard salt of the Bryan Mound dome. Unfortunately, the laboratory creep and CAVEMAN volume creep data were obtained on different caverns.

A geologic structure has been proposed for this dome [Neal et al., 1993b] that suggests an east-west anomalous zone located somewhat in the southern part of the dome. This anomalous zone has been described as a possible shear zone that is reflected in a fault in the cap rock. Of the six SPR caverns in the dome, five are former commercial caverns purchased for SPR and only one is a SPR purpose-built cavern. Since the mechanical creep properties were determined for a former commercial cavern and the volume creep closure data are for the only purpose-built cavern, little can be concluded about the correspondence of behavior. However, both the moderate material creep resistance and the volume creep closure data are consistent.

4.6 MOSS BLUFF (MB) SALT

Although the Moss Bluff dome is not the site of a SPR facility, it is located in the state of Texas, somewhat north of the Bryan Mound dome. The site is used for commercial storage operations. A four-increment creep test was performed on a single specimen from Well MB2 at the Moss Bluff dome [Wawersik, 1992]. There is no information on the geometry of the cavern.

The MB1 test results are compared to the calculated parameter integrated fit and are given in Figure 19. The fit could be considered quite good. Certainly, the initial increment shows some deviation, which is probably is not the result of any mechanical offset. The discrepancies appear to be more of the order of the uncertainty in the model and the experimental data. In any event the discrepancies are considered insignificant. As the parameter values given in Table II suggest, the Moss Bluff salt is relatively soft, nearly in the same range as the Big Hill and West Hackberry salts. It is somewhat more creep resistant than the WIPP baseline salt. At this point, there is no available information on the volume creep closure of this cavern. In addition, it appears that there is no description of the geometry of the cavern associated with Well MB2.

Although there may be information on the geologic structure of the Moss Bluff dome, we do not currently have access to such information. Also, no information is available on the relative closure rates of the cavern.

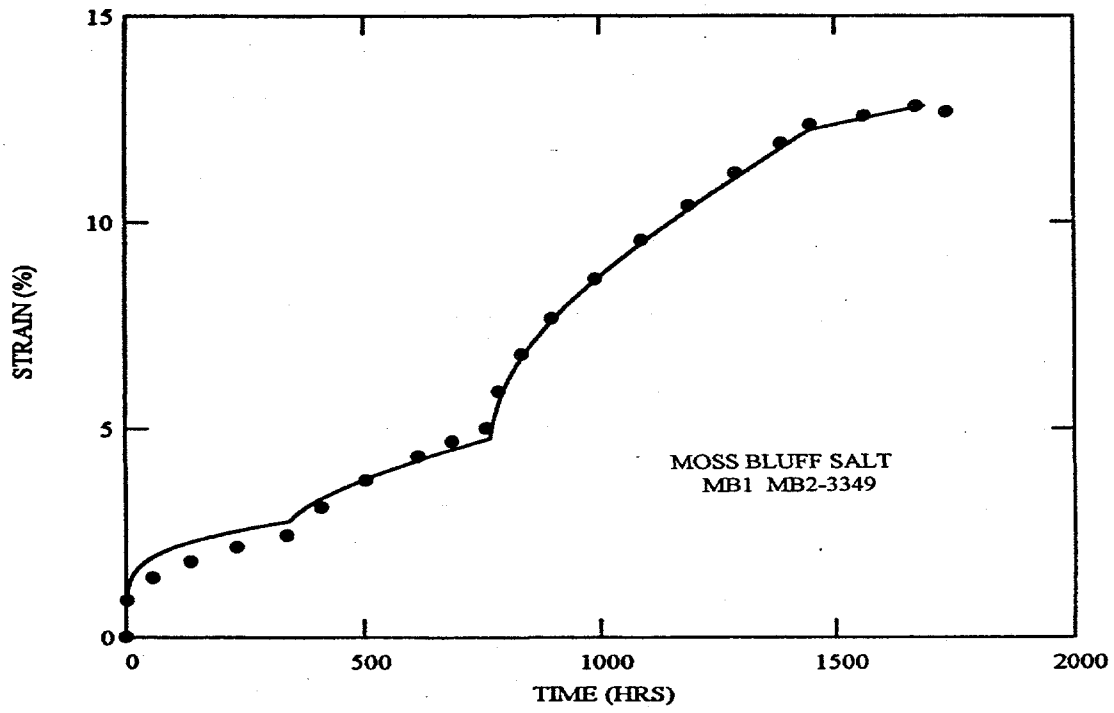

Figure 19. Calculated Fit (Solid Line) to Moss Bluff MB1 Data.

4.7 JENNINGS DOME (JD) SALT

This dome is located in the state of Louisiana near the West Hackberry dome. The Jennings dome is used for commercial storage. At this time, no specific details of the cavern geometry or siting location in the dome are available. The well at the Jennings Dome, Well LA1, provided a single test specimen, JD1. This specimen was used for a five-increment test, with the results shown in Figure 20. Again, it was not possible to obtain complete agreement and there are some discrepancies between the experimental data and the trial and error fit. Even though some offsets are apparent, principally as an over prediction in the first three increments, the parameters given in Table II provide an adequate representation of the data. Although a possible reason for the discrepancy in the first three increments is unknown, it may be the result of a vertical offset in the data which is removed during the change in conditions at the end of the third increment. The nature of the discrepancies may in fact be just the uncertainty in the model or the experimental data. Even then, the fit is probably considered acceptable. Based on this single test result, the salt from the Jennings Dome appears to be quite creep resistant, but not so much as the salt of Bryan Mound. It seems to be intermediate between the very hard salts and the very soft salts.

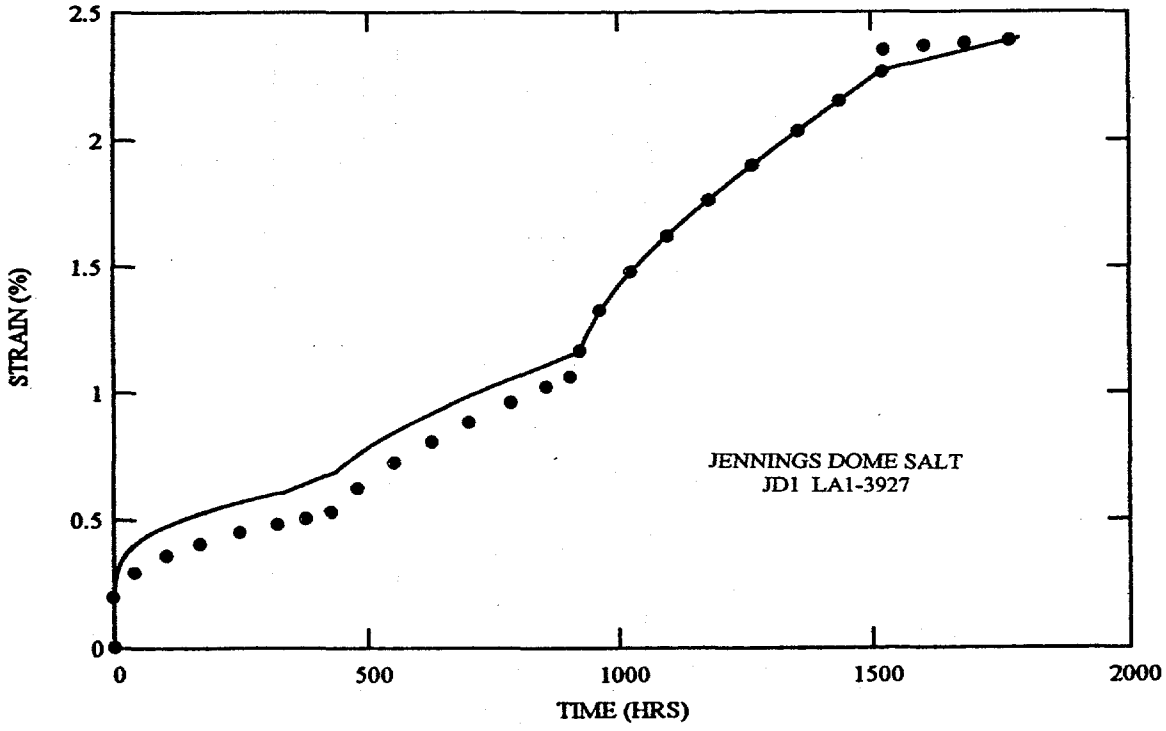

Figure 20. Calculated Fit (Solid Line) to Jennings Dome JD1 Data.

Information does not appear to be available on the geologic structure of the Jennings Dome, nor are there any data on the volume closure rates of the Jennings Dome cavern.

5.0 DISCUSSION

Perhaps the most significant consequence of the ability to determine the relative creep response of the domal salts is the possible quantitative correlation to the field behavior of caverns. While it is recognized that most existing caverns have operated adequately in the absence of any detailed geomechanical understanding of the salt, incorporation of this new knowledge into processes of siting and operation may be of benefit. Certainly, it offers another tool to aid the operator in further optimization, if possible, of cavern operation. To establish the correlation to field behavior, the CAVEMAN [Linn, 1997; Ehgartner et al., 1995] results of the analysis of SPR cavern creep closures are presented first. Then, correspondence is made to the results of the transient analysis to determine the relative creep response of the domal salts. This then suggests an interpretation about the large-scale geological structure of the domes themselves.

5.1 CAVERN VOLUME CLOSURE

In an extensive study of the pressure build-up in the caverns of the SPR, Ehgartner et al. [1995] developed a historical interpretation of cavern operation. The cavern history, in turn, can be used to predict the expected future cavern behavior. The ensuing tool is called CAVEMAN.

During standard operation of the SPR caverns, which are relatively quiescent, cavern pressure gradually increases because of the creep closure of the cavern. Periodically, the pressure is reduced by removal of fluid to maintain the operating pressure within the range acceptable to good practice and the requirements of state regulations. Through an inversion process, functions describing the geometry, stress, and material behavior that involve four adjustable parameters could reproduce the pressure build-up history. This amounts to a fitting process of the historical pressure record of a cavern. The parameters determined in the fitting process are unique to a given cavern and then become the basis for prediction of future operation of that cavern. Should a discrepancy between expected and actual pressure build-up occur, it is an indicator of potential cavern and well problems. Interestingly, the material behavior component of the method is based on the M-D constitutive equations. One of the outputs of CAVEMAN is a value of the creep closure rate of the cavern. This effective creep rate is some kind of average of the actual closure rates, which vary strongly depending upon the vertical location within the cavern and the salt dome. The vertical location determines indirectly the stress produced by the overburden and overlying salt. The effective creep closure rates of the purpose-built SPR caverns based on CAVEMAN are given in Figure 21. The four relevant salt domes for the SPR facilities are clear from the figure.

There is considerable information in Figure 21. Not only are the general closure rates significantly different between the storage caverns of the different domes, but also there are marked differences between the cavern closure rates in a given dome. Clearly, Big Hill and West Hackberry domes have the largest volume closure rates, while Bryan Mound and Bayou Choctaw domes have somewhat smaller volume closure rates. However, even here, for example, the span of closure rates of caverns in Big Hill cover a

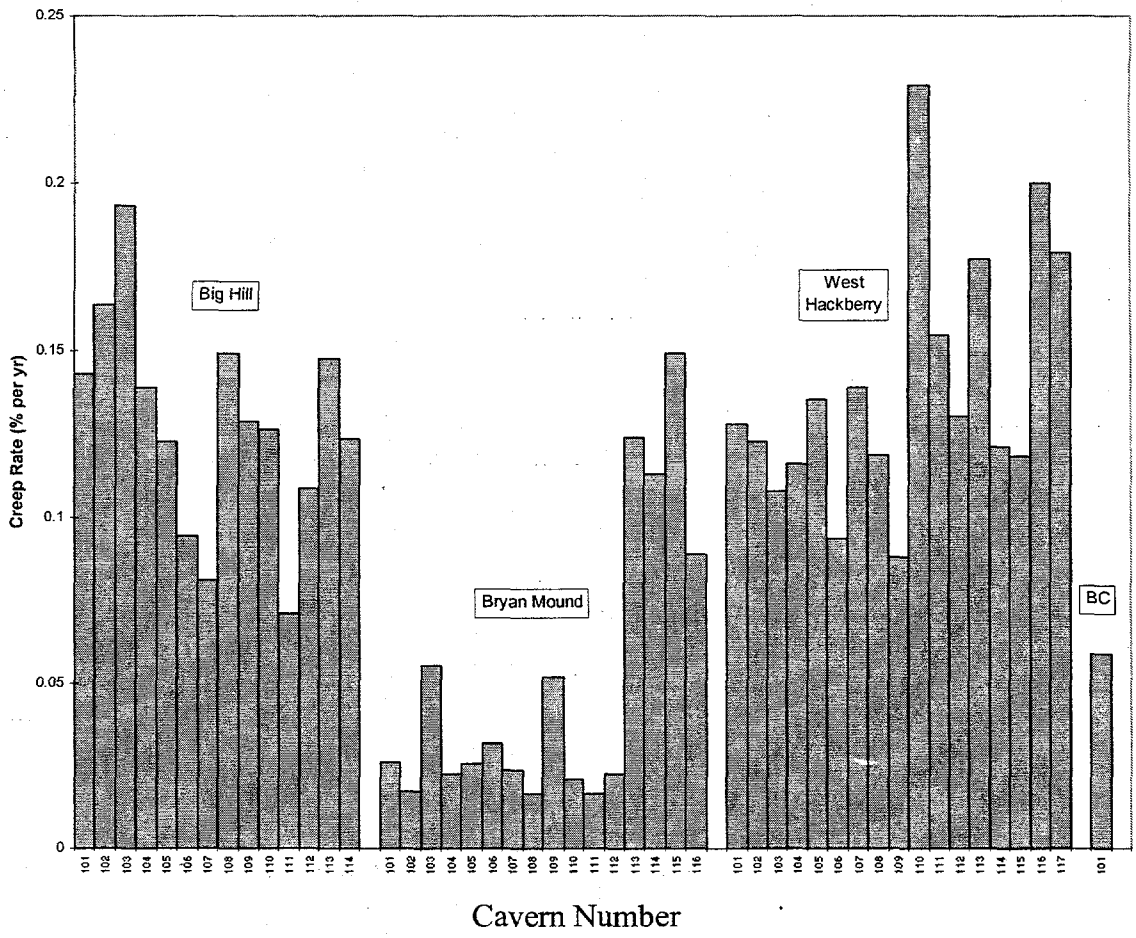

Figure 21. CAVEMAN Volume Creep Closure Rates for SPR Caverns [Linn, 1997].

considerable range, approaching as much as a factor of two. The range in closure rates of the Bryan Mound caverns is even more pronounced, varying by over a factor of four.

Certainly the quantitative closure data gives a strong indication that not all caverns respond the same within a dome, much less from one dome to another. However, the fact that the closure rates differ does not necessary, in itself, mean that the effect is the result of material behavior. This is a consequence of the nature of the effective closure rate. One of the CAVEMAN parameters is essentially a stress parameter. This stress parameter is some measure of the cavern depth within the salt dome. It reflects not only the cavern height but also the amount of overburden above the cavern. One of the other CAVEMAN parameters concerns the effective shape of the cavern. While this effect is difficult to visualize, the closure rate of equal volume caverns with different shapes could be different. That is, a conical shape would give different answers depending upon whether the apex is up or down. As a consequence, closure rates can be correctly compared only if the caverns have roughly the same geometry and have nearly the same amount of overburden and overlying salt. Fortunately, the geometry and overburdens of those caverns purpose-built for the SPR are nearly identical. Because these caverns are essentially identical in the important geometry and location aspects, the only variation

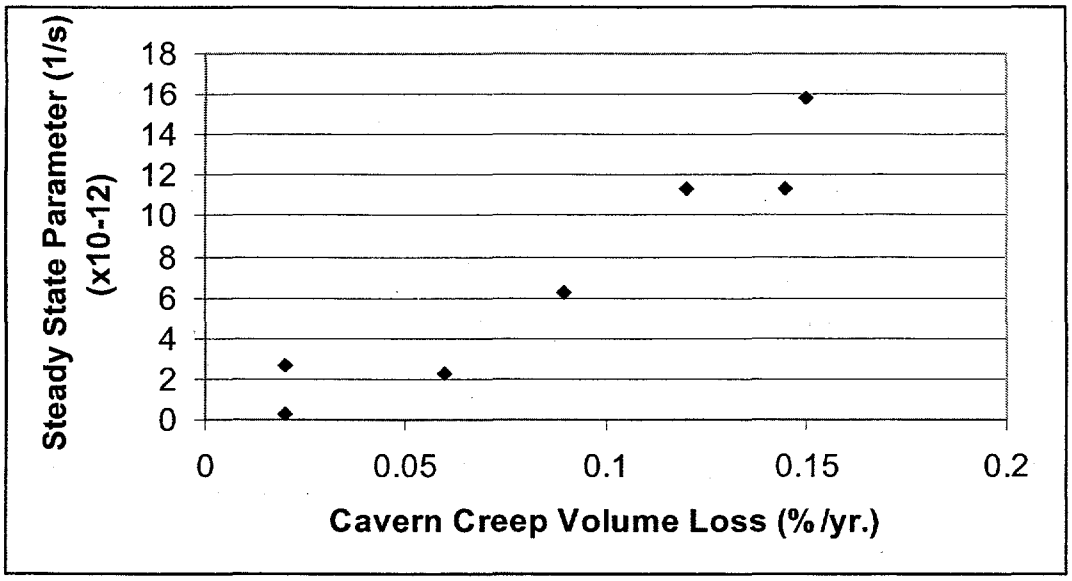

Figure 22. Steady State Creep Parameter A_2 and Cavern Creep Volume Loss.

possible is in material behavior. As a result, the differences between closure rates of the purpose-built SPR caverns shown in Figure 21 are probably solely due to differences in material response. This of course does not apply to those existing caverns initially constructed for commercially use and purchased later by the SPR.

5.2 CLOSURES RELATED TO MATERIAL REPONSE

While it is clear that characterization of the mechanical behavior of the domal salts can be quantified through analysis of the creep data, this perhaps can be extended to a broader characterization. As indicated previously, it is possible to establishing a link between laboratory material testing and the behavior of caverns in a dome. This can be carried even further to a geologic material characterization of the dome itself. Although the creep database is extremely limited, it is still possible to plot for any given cavern the value of the steady state creep parameter A_2 obtained from the transient analysis against the CAVEMAN deduced cavern volume creep rate. This plot is given in Figure 22. Even for such a small data collection, it is clear that the cavern volume loss rate is related more-or less directly to the laboratory steady state creep rate. Actually, with a larger database, the more likely dependency would be found to be logarithmic. Nevertheless, for the purposes of this study, the trend shown is probably adequate.

Even within the limitations of the quantity and quality of the creep databases available, it is remarkable that such a good correlation between laboratory data and field behavior has been obtained. It is only unfortunate that more geomechanical laboratory creep data were not obtained as a routine part of cavern construction. The apparent success of the preceding analysis might strongly suggest the desirability of requiring at least some creep data for new cavern construction and recovery of any creep data from existing caverns. In fact, it would be extremely challenging to collect creep information from all storage

caverns in a given dome. Interestingly, one of the important aspects of being able to quantify the creep response of individual caverns is that they represent discrete locations within the greater salt dome.

5.3 GEOTECHNICAL CHARACTERIZATION OF A DOME

The next step in examining how the mechanical response of caverns in a salt dome is organized is to note the relative differences in cavern volume creep loss on the plats of the facilities. This behavior is presented for two of the domes, Bryan Mound and West Hackberry. Bryan Mound SPR caverns are located in the dome as shown in Figure 23. Here, the shaded cavern locations are the purpose-built caverns with large (greater than about 0.8 %/yr.) volume creep rates. All of the other purpose-built caverns, which have a

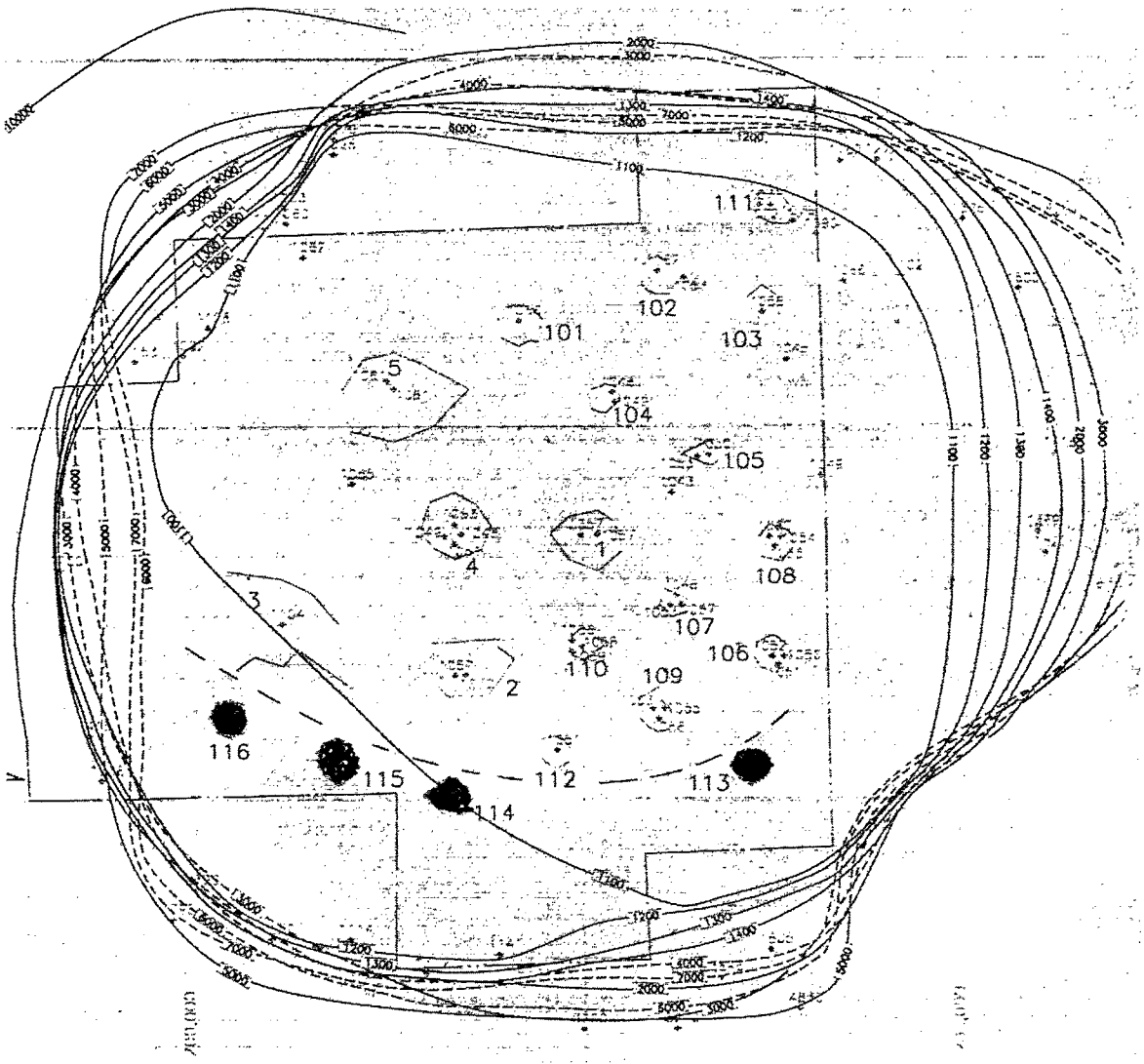

Figure 23. Plat of Bryan Mound, High (Shaded) and Low Volume Creep Caverns.

smaller closure rate (averaging less than 0.4 %/yr.) are shown as unfilled, outlined locations. The purchased caverns are also shown as unfilled outlines. A dashed line has been drawn which separates the southern limb of the dome that contains all of the caverns with high creep volume losses, specifically caverns BM113 through BM116, from the low creep volume loss caverns to the north.

On examination of the transient analysis information on the values of A_2 for the Bryan Mound dome, it becomes clear that the caverns with the soft salt are the ones with the large volume closure rates. This occurs without exception based on the very limited data available. The grouping of these less creep resistant caverns are in an east-west arc along the southern portion of the dome and may indicate that a very significant geologic feature of the Bryan Mound dome. In fact it suggests the possibility of two distinct material spines in the dome, a soft material spine to the south and a hard material spine to the north of the line of separation. It is also possible to make a further conjecture. Although it is easy to make generalizations, those caverns immediately to the north of the dashed line seem to be subject to a number of "unusual or abnormal" conditions. These conditions range from having a number of events that damaged (hanging string) casings, probably as a result of salt falls, to significant accumulations of salt with time on the cavern bottom, and further to indications of gassy conditions during construction. In Figure 23, these caverns include BM112, which experiences the greatest number of casing damage incidences and greatest quantities of bottom accumulation, and BM109 and BM106, which experience only slightly less incidences and accumulations [Munson et al., 1998]. The spine to the north may also have a concentration of impurities adjacent to the line of separation that have been postulated to cause these salt falls and bottom accumulations. Other caverns further removed to the north from the line of separation may have similar, but less severe, histories.

Although no attempt will be made to explain it, the location of the possible spines as postulated above on the basis of hard and soft salt materials does not agree qualitatively with the postulated anomalous or shear zones proposed by Neal et al. [1993a]. Clearly, with so little information, it currently seems impossible to reconcile these differences. One postulate is based primarily on surface and subsurface geology of material adjacent to the dome, while the other is based the relative material and creep closure behaviors. However, it must be noted that the postulated zones of shear may separate salt masses that are being displaced mechanically relative to one another. Potentially this mechanical displacement could involve salt of uniform creep behavior. Within this context, on the other hand, it is also possible to have two materials with different creep characteristics adjacent to each other, perhaps separated by a zone of shear.

While the above arguments are perhaps logical for the hard and soft salts of the Bryan Mound dome, the results are not nearly as clear when they are applied to the West Hackberry dome. Based on the limited amount of steady state creep data, it appears that the dome should be considered as soft salt. Even though there are $^{+}/_{-}$ 50% differences among the West Hackberry volume creep losses, these are much smaller relative differences than the factor of three or four for the Bryan Mound dome. First, it should be noted that West Hackberry rates are not separated as distinctly as are the two markedly

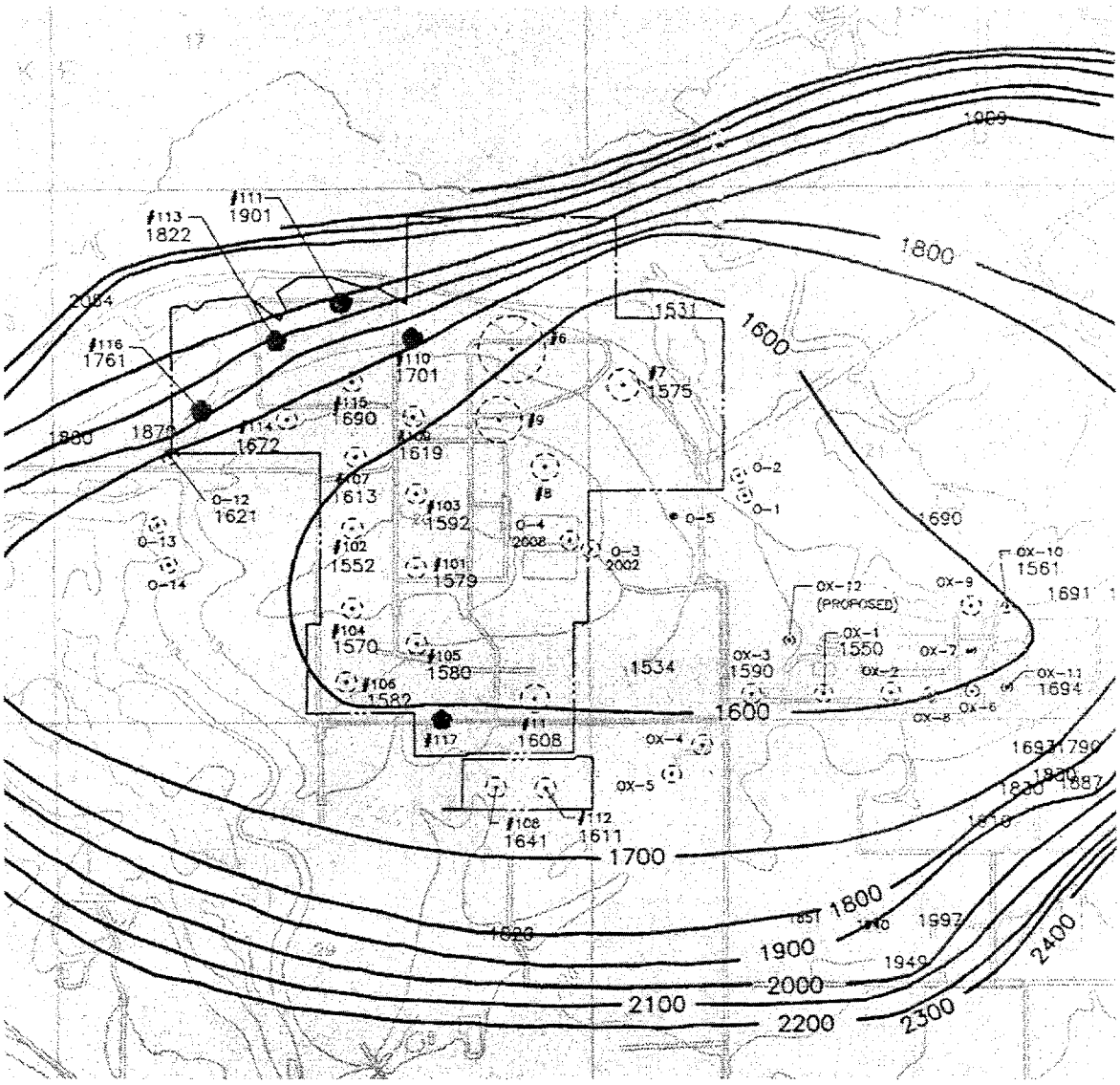

Figure 24. Plat of West Hackberry with Scattered Higher Volume Creep Loss Caverns.

different groups of Bryan Mound caverns. With this in mind, the five purpose-built West Hackberry SPR caverns with the highest volume creep loss values are shown by the filled cavern outlines in Figure 24. These caverns all have creep loss rates in excess of 0.15%/yr. Four of these purpose-built SPR caverns, WH 110, WH111, WH113, and WH116, appear along the outer rim of the northeast portion of the dome. Interestingly, the purchased cavern, WH6, for which no volume creep closure rate is available and which was determined to be soft salt with a high steady state creep rate, is also along the outer rim of the north-east portion of the dome. To further confuse this situation, the remaining high volume loss cavern, WH117, is found almost in the center of the dome, surrounded by caverns of lower volume loss. Furthermore, WH108 is known to be soft salt based on laboratory testing and is not one of the caverns with the highest volume creep loss values. Consequently, although, it is suggest that the material involved in

these five high volume loss caverns may be different than the others, it is currently impossible to suggest that they belong to a separate spine. Significantly, the cut off point selected for the high rate caverns is very arbitrary and is only 10% greater than the largest value of the remaining caverns. Perhaps, this suggests the differences in behavior of the caverns of West Hackberry are not as systematic as that of Bryan Mound. Although at this point it is somewhat risky, it is possible, based on the lack of sufficient material property differentiation, that the West Hackberry dome does not contain material spines.

The north south anomalous or shear zone postulated by Magorian et al. [1991] for West Hackberry would essentially bisect the SPR cavern field. While this geologic based observation may suggest a mechanical displacement domal spine structure, the material creep response and cavern creep closure data do not suggest a related material structure.

At this point in this study, the picture is extremely mixed of how material properties, specifically the creep properties, reflect the structure of a salt dome. Clearly, various locations in the dome can have markedly different creep characteristics, as appears to be the case in the Bryan Mound dome. Here, the creep resistant salt seems to be concentrated in one region of the dome and the less creep resistant salt in another, to form what may be distinct material spines. For West Hackberry it appears volume creep rates vary by a factor of two over the dome. Even though some, but not all, of the highest volume creep caverns occur in an arc along the rim of the dome, there doesn't seem to be enough difference to suggest possible material spines. Part of the problem in assigning geological significance is due to the mixed nature of the evidence. We have the two quantities, the limited laboratory creep tests and the field volume creep loss quantities. In the case of Bryan Mound, the two measurements of material response correspond, indicating that the marked differences in calculated field creep volume losses are matched by the differences in measured laboratory creep parameters. In West Hackberry, however, the supposition from the limited laboratory creep parameters is the dome is all soft salt, without any marked evidence from the variation in the volume creep loss values to indicate otherwise.

6.0 CONCLUSIONS

From the framework provided by the Multimechanism-Deformation (M-D) constitutive description of salt creep, it is possible to obtain the model parameters through trial and error fits to very limited creep databases. Initially, the framework provided only the form of the steady state creep response as the bound for conventional and incremental test data. The results of this steady state analysis suggested that domal salts were either "hard" or "soft" salts depending upon their creep resistance. However, shortcomings of this steady state analysis method permitted some data to obscure the actual steady state response of other data. Consequently, it was necessary to develop a more detailed transient analysis method based on the direct integration of the M-D equations. Using this detailed method, individual creep tests, either conventional or incremental, could be fitted through trial and error to obtain the material sensitive parameters best describing the test material. Although there are numerous model parameters that must be considered, only three are significantly material sensitive to become involved in the fitting technique. These parameters are the steady state creep rate as specified through the structure parameter, A_2, the transient strain limit as determined by K_0, and the workhardening curvature as given by α. When this transient analysis was completed, the same hard and soft salt designations were observed as previously; however, Bryan Mound dome was found to contain both types of salt. These transient analyses of laboratory creep data supports the cavern volume creep closure results found from the analyses of CAVEMAN, a fitting program for using the history of pressure build-up in quiescent caverns to predict future cavern response. Results of the transient analysis of very sparse laboratory creep databases suggest that these data may be a valuable tool in the selection of candidate cavern locations for new caverns or in the understanding of the operational characteristics of existing caverns.

With the knowledge of the creep volume closure and the laboratory creep response of the various SPR caverns, it was possible to place this information in the geological context of the salt dome. As a consequence, it is believed that the Bryan Mound salt dome consists of at least two material spines, one of creep resistant salt and one of less creep resistant salt. This is supported both by the relative creep volume closures and the relative creep resistance of the salts. The West Hackberry SPR caverns, while showing some deviation in the creep response, never-the-less are all in soft salt, with little apparent possibility of material spines. Likewise, the other SPR facilities in the Bayou Choctaw and Big Hill salt domes suggest a more uniform material makeup, equivalent to West Hackberry.

REFERENCES

Chan, K.S., D.E. Munson, A.F. Fossum, and S.R. Bodner, 1996. Inelastic Flow Behavior of Argillaceous Salt, Int'l J. Damage Mech., **5**, 292-314.

Chan, K.S., D.E. Munson, A.F. Fossum, and S.R. Bodner, 1998. A Constitutive Model for Representing Coupled Creep, Fracture, and Healing in Rock Salt, Proc. 4th Conf. on the Mech. Behavior of Salt, Trans Tech Publications, Clausthal-Zellerfeld, Germany, 221-234.

DeVries, K.L., 1988. Viscoplastic Laws for Avery Island Salt, Report for Stone Webster, RSI-0333, RE/SPEC, Inc., Rapid City, SD.

Ehgartner, B., S. Ballard, M. Tavares, S. Yeh, T. Hinkebein, and R. Ostensen, 1995. A Predictive Model for Pressurization of SPR Caverns, Proc. SMRI Fall Meeting 1995, San Antonio, TX, Solution Mining Research Institute, Deerfield, IL.

Kupfer, D.H., 1963. Structure of Salt in Gulf Coast Domes, 1st Symp. on Salt, N. Ohio Geol. Soc., Cleveland, OH, pp.215-225.

Linn, J.K., 1997. Letter to R.E. Myers, November 25, 1997 with attachment on "SPR Ullage Study" by B.L. Ehgartner, Sandia National Laboratories, Albuquerque, NM.

Looff, K.M., and K.M. Looff, 1999. Possible Geologic Influence on Salt Falls Associated with the Storage Caverns at Bryan Mound, Brazoria County, Texas, Proc. SMRI Spring Meeting 1999, Las Vegas, TX, Solution Mining Research Institute, Encinitas, CA.

Magorian, T.R. J.T. Neal, S. Perkins, Q.J. Xiao, and K.O. Byrne, 1991. Strategic Petroleum Reserve (SPR) Additional Geologic Site Characterization Studies West Hackberry Salt Dome, Louisiana, SAND90-1224, Sandia National Laboratories, Albuquerque, NM.

Mellegard, K.D., P.E. Senseny, and F.D. Hansen, 1983. Quasi-Static Strength and Creep Characteristics of 100-mm-Diameter Specimens of Salt from Avery Island, Louisiana, Technical Report ONWI-250, Office of Nuclear Waste Isolation, Battelle, Columbus, OH.

Mellegard, K.D., and T.W. Pfeifle, 1996. Laboratory Creep test on Domal Salt from Weeks Island, Louisiana, Topical Report RSI-0756, RE/SPEC Inc., Rapid City, SD.

Munson, D.E., 1979. Preliminary Deformation-Mechanism Map for Salt (with Application to WIPP), SAND70-0079, Sandia National Laboratories, Albuquerque, NM.

Munson, D.E., and P.R. Dawson, 1982. A Transient Creep Model for Salt during Stress Loading and Unloading, SAND82-0962, Sandia National Laboratories, Albuquerque, NM.

Munson, D.E., A.F. Fossum, and P.E. Senseny, 1989. Advances in Resolution of Discrepancies between Predicted and Measured In Situ WIPP Room Closures, SAND88-2948, Sandia National Laboratories, Albuquerque, NM.

Munson, D.E., 1997. Constitutive Model of the Creep of Rock Salt Applied to Underground Room Closure, Int'l. J. Rock Mech. and Min. Sci. & Geomech. Abstr., **34** (2), 233-248.

Munson, D.E., and B.L. Ehgartner, 1997. Memorandum to J.K. Linn, July 11, 1997. "Comparison of Steady State Creep Response of Weeks Island and WIPP Salt," Sandia National Laboratories, Albuquerque, NM.

Munson, D.E., M.A. Molecke, J.T. Neal, A.R. Sattler, and R.E. Myers, 1998. Strategic Petroleum Reserve Caverns Casing Damage Update 1997, SAND98-0090, Sandia National Laboratories, Albuquerque, NM.

Munson, D.E., 1998. Analysis of Multistage and Other Creep Data for Domal Salts, SAND98-2276, Sandia National Laboratories, Albuquerque, NM.

Neal, J.T., T.R. Magorian, R.L. Thoms, W.J. Autin, R.P. McCulloh, S. Denzler, and K.O. Byrne, 1993a. Anomalous Zones in Gulf Coast Salt domes with Special Reference to Big Hill, TX, and Weeks Island, LA, SAND92-2283, Sandia National Laboratories, Albuquerque, NM.

Neal, J.T., T.R. Magorian, K.O. Byrne, and S. Denzler, 1993b. Strategic Petroleum Reserve (SPR) Additional Geologic Site Characterization Studies Bayou Choctaw Salt Dome, La, SAND92-2284, Sandia National Laboratories, Albuquerque, NM.

Neal, J.T., T.R. Magorian, and S. Ahmad, 1994. Strategic Petroleum Reserve (SPR) Additional Geologic Site Characterization Studies Bryan Mound Salt Dome, Texas, SAND94-2331, Sandia National Laboratories, Albuquerque, NM.

Ortiz, T.S., 1980. Strategic Petroleum Reserve (SPR) Geological Summary Report Weeks Island Salt Dome, SAND80-1323, Sandia National Laboratories, Albuquerque, NM.

Wawersik, W.R., D.W. Hannum, and H.S. Lauson, 1980a. Compression and Extension Data for Dome Salt from West Hackberry, Louisiana, SAND79-0688, Sandia National Laboratories, Albuquerque, NM.

Wawersik, W.R., D.J. Holcomb, D.W. Hannum, and H.S. Lauson, 1980b. Quasi-Static and Creep Data for Dome Salt from Bryan Mound, Texas, SAND80-1434, Sandia National Laboratories, Albuquerque, NM.

Wawersik, W.R., and D.H. Zeuch, 1984. Creep and Creep Modeling of Three Domal Salts – A Comprehensive Update, SAND84-0568, Sandia National Laboratories, Albuquerque, NM.

Wawersik, W.R., 1985. Memorandum to R.R. Beasley, January 3, 1985, "Creep Measurements on Big Hill Salt," Sandia National Laboratories, Albuquerque, NM.

Wawersik, W.R., 1992. Indicator Tests for the Creep of Rock Salt from Borehole Moss Bluff 2, Moss Bluff Dome, Texas, SAND92-2122, Sandia National Laboratories, Albuquerque, NM.

Wawersik, W.R., and D.J. Zimmerer, 1994. Triaxial Creep Measurements on Rock Salt from the Jennings Dome, Louisiana, Borehole LA-1, Core #8, SAND94-1432, Sandia National Laboratories, Albuquerque, NM.

DISTRIBUTION

U.S. DOE SPR PMO (8)
Strategic Petroleum Reserve
900 Commerce Road East
New Orleans, LA 70123
Attn: G. B. Berndsen, FE-443.1
R. E. Myers, FE-4421 (5)
W. Poarch, FE-4421
J. Culbert, FE-443

U.S. Department of Energy (2)
Strategic Petroleum Reserve
1000 Independence Avenue SW
Washington, D.C. 20585
Attn: D. Johnson, FE-42
D. Buck, FE-42

DynMcDermott (7)
850 South Clearview Parkway
New Orleans, LA 70123
Attn: K. E. Mills, EF-25
G. Hughes, EF-22
J. McHenry, EF-21
J. Farquhar, DM-21
F. Tablada, EF BC
H. Bakhtiari, EF BM
J. Sanner, EF WH

RE/SPEC Inc.
3824 Jet Drive
Rapid City, SD 57709-0725
Attn: T. Pfeifle

Prof. Michel Aubertin
Ecole Polytechnique de Montreal
P.O. Box 6079, Station Centre-ville
Montreal, Quebec
H3C 3A7
CANADA

Prof. Pierre Berest (3)
Laboratoire de Mecanique des Solides
Ecole Polytechnique
Palaiseau
FRANCE 91128

Dr. Manfred Wallner (3)
Bundesanstalt fur Geowissenschaften
und Rohstoffe
Postfach 510 153
D-30631 Hannover
GERMANY

Sandia Internal: (36)

MS 0431 S. G. Varnado, 6200
MS 0701 L. E. Shepard, 6100
MS 0706 J. K. Linn, 6113 (10)
MS 0706 D. E. Munson, 6113 (10)
MS 0706 6113 Staff (8)
MS 0751 N. S. Brodsky, 6114
MS 0847 A. F. Fossum, 9117
MS 9018 Central Technical Files, 8940-2
MS 0899 Technical Library, 4916 (2)
MS 0612 Review and Approval Desk, 4912, For DOE/OSTI